SILAC-based quantitative proteomics reveals pleiotropic, phenotypic modulation in primary murine macrophages infected with the protozoan pathogen Leishmania donovani

Despina Smirlis, Florent Dingli, Pascale Pescher, Eric Prina, Damarys Loew, Najma Rachidi, Gerald Späth

SILAC-based quantitative proteomics reveals pleiotropic, phenotypic modulation in primary murine macrophages infected with the protozoan pathogen *Leishmania donovani*

Despina Smirlis[1,2*], Florent Dingli[3], Pascale Pescher[1], Eric Prina[1], Damarys Loew[3], Najma Rachidi[1], Gerald F. Späth[1*]

1. Institut Pasteur and Institut National de Santé et Recherche Médicale INSERM U1201, Unité de Parasitologie Moléculaire et Signalisation, Paris, France
2. Hellenic Pasteur Institute, Molecular Parasitology Laboratory, Athens, Greece
3. Laboratoire de Spectrométrie de Masse Protéomique, Centre de Recherche, Institut Curie, Université de recherche PSL, Paris, France

Corresponding authors:
Despina Smirlis, Molecular Parasitology Laboratory, Hellenic Pasteur Institute, 127 Vas. Sofias Ave., 11521, Athens, Greece, telephone: (+30) 2016478841, fax: (+30) 210 64 78853, e-mail: penny@pasteur.gr
Gerald F. Spaeth: Institut Pasteur and Institut National de Santé et Recherche Médicale INSERM U1201, Unité de Parasitologie Moléculaire et Signalisation, 25 Rue Du Docteur Roux, 75015, Paris, France, telephone: (+33)140613858, fax: (+33)14568.8332; e-mail: gerald.spaeth@pasteur.fr

Acknowledgements
This work was supported by the Institute Pasteur Transverse Research Programs [PTR, grant no.: PTR539], the French Government's Investissement d'Avenir Program, Labex Integrative Biology of Emerging Infectious Diseases [grant no.: ANR-10-LABX-62-IBEID], and by "Région Ile-de-France" [grant no.: 2013-2-EML-02-ICR-1] and Fondation pour la Recherche Médicale grants [grant no.: DGE20121125630].

ABSTRACT

Leishmaniases are major vector-borne tropical diseases responsible for great human morbidity and mortality, caused by protozoan, trypanosomatid parasites of the genus *Leishmania.* In the mammalian host, parasites survive and multiply within mononuclear phagocytes, especially

macrophages. However, the underlying mechanisms by which *Leishmania* spp affect their host are not fully understood**.** Herein, proteomic alterations of primary, bone marrow-derived BALB/c macrophages are documented after 72 h of infection with *Leishmania donovani* insect-stage promastigotes, applying a SILAC-based, quantitative proteomics approach. The protocol was optimised by combining strong anion exchange and gel electrophoresis fractionation that displayed similar depth of analysis (combined total 6189 mouse proteins). Our analyses revealed 86 differentially modulated proteins (35 showing increased and 51 decreased abundance) in response to *Leishmania donovani* infection. The proteomics results were validated by analysing the abundance of selected proteins. Intracellular *Leishmania donovani* infection led to changes in various host cell biological processes, including primary metabolism and catabolic process, with a significant enrichment in lysosomal organisation. Overall, our analysis establishes the first proteome of *bona fide* primary macrophages infected *ex vivo* with *Leishmania donovani*, revealing new mechanisms acting at the host/pathogen interface.

Keywords: quantitative proteomics, bone marrow-derived macrophages, *Leishmania donovani*, SILAC, LC-MS/MS

INTRODUCTION

The leishmaniases include a group of diseases caused by more than 21 protozoan species of the trypanosomatid genus *Leishmania,* which are transmitted by the bite of phlebotomine sandflies [1]. These diseases, prevalent in 98 countries, have different clinical outcomes that range from localised skin ulcers (cutaneous leishmaniasis) to lethal systemic disease (visceral leishmaniasis, VL)[2]. VL is the most serious form of the disease, with 200 000 to 400 000 new cases documented every year [2] and a lethal outcome if left untreated. VL is caused mainly by strains of the *Leishmania (L.). donovani* complex and is characterised by systemic symptoms, such as fever and weight loss [3].

All *Leishmania* parasites share a digenetic life cycle and live either as extracellular, motile promastigotes within the midgut of a sand fly vector, or as intracellular, non-motile

amastigotes in professional phagocytes, with macrophage phagolysosomes representing the primary niche for proliferation [4]. These phagocytic mononuclear cells carry important, immuno-regulatory functions and accordingly can differentiate into phenotypically distinct subtypes [5], including pro-inflammatory M1 cells with microbicidal properties and alternatively activated, anti-inflammatory M2 cells involved in tissue repair (reviewed in [6]). These M1 and M2 phenotypes represent the extremes of a continuous spectrum of polarisation states [7]. Even though both the initial *Leishmania* infection through the bite of infected sand flies and the later acute stages of the disease are characterised by inflammation of the infected tissue [8, 9], *Leishmania* thrives in these environments by efficiently dampening the pro-inflammatory response of its infected host cell, possibly by exploiting developmental programs underlying macrophage phenotypic plasticity [10].

The prevention of *Leishmania* clearance and persistent infection of macrophages is governed by the expression of specific parasite virulence factors, such as highly abundant parasite surface glycolipids [lipophosphoglycan (LPG) and glycoinositol phospholipids (GIPLs)], or the GPI anchored metalloprotease, GP63 [11-15]. These and other factors have been shown to remodel the macrophage phenotype to establish permissive conditions for *Leishmania* intracellular survival. Initially, following entry into the macrophage, *L. donovani* promastigotes delay phagosomal/lysosomal fusion and phagosome maturation [16-18], and subsequently modify host cell signaling and metabolic processes, inhibit apoptosis and suppress antigen presentation (reviewed in [10]).

However, this ideal concept of 'macrophage deactivation' upon *Leishmania* infection is clearly an oversimplification, as the macrophage response to infection under clinically more relevant conditions can depend on many parameters, including the host cell differentiation state, the tissue context, and parasite species or even strain [19, 20]. Systems-level, 'omics' approaches revealed the complex interface between the parasite and the macrophage and shed important new light on the host cell response to *Leishmania* infection, particularly at the transcript level [8, 9, 19, 21-27]. However, transcript abundance does not always correlate with protein levels and thus may not give an accurate picture of the cellular phenotype. Proteome

analyses certainly allows for a more relevant functional insight, but the few proteomics screens - reviewed in Veras & Menezes, 2016 [28] - were performed on *Leishmania* infected cells using either immortalised, macrophage-like cell lines [29, 30] known to be phenotypically and functionally different from *bona fide* macrophages [31-34], or a semi-quantitative approach based on spectral counting [20] that lacks quantitative performance [35]. Here we overcame these limitations and for the first time quantified proteomic changes in primary, bone marrow-derived macrophages (BMDMs) after 72 h of infection with virulent *L. donovani* promastigotes using stable isotope labeling by amino acids in cell culture (SILAC). SILAC, a technique that relies on the metabolic replacement of a given natural amino acid (referred to as 'light') with a non-radioactive, stable isotope (referred to as 'heavy') [36], is considered one of the most accurate quantitative approaches when using cell culture systems to study dynamics of biological processes [35, 36]. Our analysis confirms known signatures of infected macrophages, but also provides new insight into *L. donovani*-induced phenotypic changes of primary macrophages and mechanisms of intracellular parasite survival acting at the host/pathogen interface.

MATERIALS AND METHODS

Ethics statement

All animal experiments complied with the ARRIVE guidelines and were carried out according to the EU Directive 2010/63/EU for animal experiments. All animals were housed in an A3 animal facility of Institut Pasteur (Paris). Housing and conditions were in compliance with the protocol approved by the Institut Pasteur (Paris) ethical committee for animal experimentation (CETEA: C2TEA 89)) and procedures were conducted in agreement with the project licenses HA0005and#10587, issued by the Institut Pasteur CETEA and the Ministère de l'Enseignement Supérieur de la Recherche et de l'Innovation (MESRI) respectively.

Leishmania culture, BMDM differentiation and infection

L. donovani strain 1S2D (MHOM/SD/62/1S-CL2D obtained from Henry Murray (Weill Cornell Medical College, New York, USA)) was maintained in female RjHan:AURA golden Syrian hamsters between four and six weeks of age (Janvier Labs) by serial *in vivo* passaging. Amastigotes were purified from hamster spleens as described [37] and differentiated into promastigotes in culture that were maintained for no more than five *in vitro* passages. Parasites were cultivated at 26°C in fully supplemented M199 medium (10% FCS, 25 mM HEPES, 4 mM $NaHCO_3$, 1 mM glutamine, 1 x RPMI 1640 vitamin mix, 0.2 µM folic acid, 100 µM adenine, 7.6 mM hemin, 8 µM biopterin, 50 U ml^{-1} of penicillin and 50 µg ml^{-1} of streptomycin, pH7.4).

Bone marrow cell suspensions were recovered from tibias and femurs of BALB/c mice (Janvier) and suspended in bacteriologic Petri dishes (Greiner, Germany) at a concentration of $1.35x10^6$ ml^{-1} in complete medium i.e. RPMI 1640 supplemented with 50 µM β-mercaptoethanol, 15% heat-inactivated fetal calf serum (GIBCO), 50 U ml^{-1} of penicillin and 50 µg ml^{-1} of streptomycin and 75 ng mL^{-1} of macrophage Colony Stimulating Factor-1 (mCSF-1) (Immunotools). Cells were incubated at 37°C and 5% CO_2. Three days after plating, 0.4 volume of fresh complete medium was added to the cells. Six days later, adherent bone marrow-derived macrophages (BMDMs) were washed with Dulbecco's phosphate buffered solution (PBS). Cells were detached by incubation with Dulbecco's PBS without Ca^{2+} and Mg^{2+} (Biochrom AG, Berlin, Germany) containing 25 mM EDTA for 30min at 37°C.

For *Leishmania* infection, recovered BMDMs were plated in flat-bottom, 6-well plates (Tanner, Switzerland) at a density of $4x10^6$ cells per well and were maintained in complete medium. Six hours after plating, macrophages were infected with $4x10^7$ *L. donovani* stationary phase promastigotes (multiplicity of infection of 10:1, *in vitro* passage 2 after differentiation from splenic amastigotes) for 4 h and incubated at 37°C in a 5% CO_2. Following infection, macrophages were washed four times with PBS to remove free promastigotes. Infected and non-infected macrophages were then maintained for 72 h in complete medium containing only 25 ng mL^{-1} mCSF-1.

SILAC labelling and sample preparation

For labelling cells by SILAC, equal numbers of BMDMs were differentiated and cultured as described above, but using RPMI 1640 without Lysine and Arginine (Thermo Fisher Scientific) that was supplemented either with natural amino acids (L-Lysine, 0.274 mM; L-Lysine, 1.15 mM; Arginine, 1.15 mM) to obtain "light" cells (referred to as control) or with amino acid isotopes $^{2}H_{4}$-Lysine (Lys4) and $^{13}C_{6}$-Arginine (Arg6) at the same concentrations to obtain "heavy" cells (referred to as labelled) (Thermo Scientific). Fetal calf serum (GIBCO) was dialysed over night against 100 volumes of sterile PBS, followed by two new rounds of 3 h dialysis, each against a low cutoff membrane (3.5 kD, Gebaflex). The light or heavy RPMI 1640 was supplemented with 15% (v/v) of dialysed and filter-sterilised serum, 50 μM β-mercaptoethanol, 50 U ml^{-1} penicillin, 50 μg ml^{-1} streptomycin, and 75 ng mL^{-1} of mCSF-1.

BMDMs cultivated in SILAC medium were washed three times in PBS and were lysed with a buffer containing 8 M urea, 50 mM ammonium bicarbonate pH7.5, one tablet per 10 ml of cOmplete™ Protease Inhibitor Cocktail tablets (Sigma), and one tablet of the phosphatase inhibitor cocktail PhosSTOP (Roche). Cell extracts were incubated on ice 30 min, sonicated 5 min, and centrifuged 15 min at 14,000 *g* to eliminate cell debris. Proteins were quantified in the supernatants using the RC DC™ protein assay kit (Bio-Rad), according to the manufacturer's instructions. For protein identification and quantification, control infected were mixed with labeled non-infected and labeled infected were mixed with control non-infected at an equal ratio.

SILAC Sample processing

Samples supernatants as processed above were fractionated by two different methods: (i) polyacrylamide gel electrophoresis fractionation (GEL) and (ii) Strong Anion eXchange (SAX). For GEL fractionation, mixed samples were separated by polyacrylamide gel electrophoresis (PAGE) with the use of Invitrogen NuPAGE 10% Bis-Tris 1.0mm*10 Well

gels. Proteins were recovered from 9 gel slices following in-gel digestion as described in standard protocols. Briefly, following the SDS-PAGE and washing of the excised gel slices, proteins were reduced by adding 10 mM DTT (Sigma Aldrich) prior to alkylation with 55 mM iodoacetamide (Sigma Aldrich). After washing and dehydrating the gel pieces with 100% acetonitrile, trypsin (Sequencing Grade Modified, Roche Diagnostics) was added and proteins were digested overnight in 25 mM ammonium bicarbonate at 30°C.

SAX-based samples were digested in solution prior to fractionation of peptides. Briefly, the protein extracts obtained by urea extraction were mixed at a 1:1 ratio and subjected to the following process: First, samples were reduced using 10 mM DTT, alkylated with 55 mM iodoacetamide and digested using Trypsin overnight. Second, peptides were desalted through Sep-Pak C18 cartridges (Waters) and dried down prior to their fractionation. Peptide fractionation was carried out through SAX using in-house prepared microcolumns (anion exchange disks, Empore) and a Britton - Robinson buffer (20 mM acetic acid, 20 mM phosphoric acid, 20 mM boric acid) at six decreasing pH values (11, 8, 6, 5, 4, 3) for the elution of peptides [38].

Samples were loaded onto homemade C18 SepPak-packed StageTips for desalting (principle by stacking one 3M Empore SPE Extraction Disk Octadecyl (C18) and beads from SepPak C18 Cartridge (Waters) into a 200 µL micropipette tip). Peptides were eluted with 40/60 MeCN/H_2O + 0.1% formic acid and lyophilysed under vacuum. Desalted samples were reconstituted in injection buffer (2% MeCN, 0.3% TFA) for LC-MS/MS analysis.

LC-MS/MS analysis

Online liquid chromatography (LC) was performed with an RSLCnano system (Ultimate 3000, Thermo Scientific) coupled online to an Orbitrap Fusion Tribrid mass spectrometer (MS, Thermo Scientific). Peptides were trapped on a C18 column (75 µm inner diameter × 2 cm; nanoViper Acclaim PepMap^{TM} 100, Thermo Scientific) with buffer A (2/98 MeCN/H_2O in 0.1% formic acid) at a flow rate of 4.0 µL/min over 4 min. Separation was performed on a 50 cm x 75 µm C18 column (nanoViper Acclaim PepMap^{TM} RSLC, 2 µm, 100Å, Thermo

Scientific) regulated to a temperature of 55°C with a linear gradient of 5% to 25% buffer B (100% MeCN in 0.1% formic acid) at a flow rate of 300 nL/min over 100 min for the SAX and the GEL samples. Full-scan MS was acquired in the Orbitrap analyzer with a resolution set to 120,000, a mass range of m/z 400–1500 and a 4×10^5 ion count target. Tandem MS was performed by isolation at 1.6 Th with the quadrupole, HCD fragmentation with normalised collision energy of 30, and rapid scan MS analysis in the ion trap. The MS^2 ion count target was set to 2×10^4 and only those precursors with charge state from 2 to 7 were sampled for MS^2 acquisition. The instrument was run in top speed mode with 3 s cycles

MS Data Processing and Protein Identification

Data were searched against the Swiss-Prot *Mus musculus* (012016) and *L. donovani* (20150914) databases, using Sequest^{HT} through Thermo Scientific Proteome Discoverer (v 2.1). The mass tolerances in MS and MS/MS were set to 10 ppm and 0.6 Da, respectively. We set carbamidomethyl cysteine, oxidation of methionine, N-terminal acetylation, heavy $^{13}C_6$-Arginine (Arg6) and $^{2}H_4$-Lysine (Lys4) as variable modifications. We set specificity of Trypsin digestion and allowed two missed cleavage sites.

The resulting files were further processed by using myProMS (v 3.5) [39]. The Sequest HT target and decoy search result were validated at 1% false discovery rate (FDR) with Percolator. For SILAC-based protein quantification, peptides XICs (Extracted Ion Chromatograms) were retrieved from Thermo Scientific Proteome Discoverer. Global Median Absolute Deviation (MAD) normalisation was applied on the total signal to correct the XICs for each biological replicate. Protein ratios were computed as the geometrical mean of related peptides. To estimate ratio significance, a t-test was performed with the R package limma [40] and the false discovery rate has been controlled using the Benjamini-Hochberg procedure [41].

RNA isolation and RT qPCR

Total RNA was isolated from macrophages using the Nucleospin RNA isolation kit (MACHEREY-NAGEL GmbH, Germany) according to the manufacturers' instructions. The

integrity of the RNA was assessed using the Agilent 2100 Bioanalyzer system. For RNA reverse transcription to first strand cDNA, 1 µg of total RNA was mixed with random hexamers (Roche Diagnostics) and MMLV-RT reverse transcriptase (Moloney Murine Leukemia Virus, Invitrogen Life Technologies), and the reaction was carried according to the manufacturer's instructions. qPCR was performed with the QuantiTect SYBR Green kit (Qiagen) according to the manufacturers' instructions in a 10 µL reaction mixture containing 1 µL cDNA template and 0.5 µM forward/ reverse primers and 5 µl 2x QuantiTect master mix. The reactions were performed in triplicates in white FrameStar® 384 PCR plates (4titude) on a LightCycler® 480 system (Roche Diagnostics, Meylan, France) and gene expression analysis was performed with the use of qBase [42]. The primers used are listed in **Table S1**. Analysis of PCR data and normalisation over the reference genes Yhwaz and RpL19, were performed as previously described [43].

Western blot analysis

Total protein extracts were separated on 4–12% Bis-Tris NuPAGE® gels (Invitrogen) and blotted onto polyvinylidene difluoride (PVDF) membranes (Pierce). Western blot analyses were performed as previously described [44]. The following primary antibodies were used at 1:1000 dilution: rabbit anti-GSTm (Abcam, ab178684), anti-Asah-1 (ab74469), anti-Rab3IL1 (Abcam, ab98839), anti-Plxna1 (Abcam, ab23391), anti-Hmox-1 (Abcam, ab13243) and anti-Ctsd (Abcam, ab75852) and the monoclonal anti-β actin 13E5 (Cell Signaling Technologies, #4970). The anti-rabbit and anti-mouse secondary antibodies (Pierce) were diluted 1:20000. Blots were developed using SuperSignal™ West Pico (Pierce) according to the manufacturer's instructions. Western blots were quantified with Image J software.

Counting of intracellular parasites

Infected and non-infected macrophages plated on coverslips were fixed for 20 minutes at RT with 4% (w/v) parafolmaldehyde (PFA) in phosphate buffered saline (PBS) and incubated for

15 min with PBS containing the nuclear dye Hoechst 33342 (0.5 µg/ml). Excess dye was removed by rinsing coverslips in PBS before mounting on a microscope slide using Mowiol (Sigma-Aldrich). Two different cover slips per condition were analysed with a Leica DMI6000B microscope or an inverted microscope equipped with ApoTome (ZEISS).

Functional enrichment analysis

GO default annotations were parsed from the available NCBI GO information (http://www.ncbi.nlm.nih.gov/Ftp/), using as background the whole annotation from Uniprot *Mus musculus* reference proteome (UP000000589). The GO enrichment analysis for biological process, molecular function and cellular component was performed using the proteins listed in **Table 1** and **2** as input. The multiple testing correction was selected to the Benjamini and Hochberg false discovery rate at a significance level of 0.01. Results were visualised using the Cytoscape 3.5.1 software package [45] and the BinGO plug-in [46].

RESULTS AND DISCUSSION

Metabolic labeling of BMDMs in SILAC medium and experimental workflow for SILAC experiments

First, we tested the capacity of *L. donovani* promastigotes to infect and proliferate within control and isotope-labelled BMDMs. Macrophages at day 6 post-differentiation in SILAC culture medium were infected at a parasite-to-macrophage ratio of 10:1 with *L. donovani* promastigotes at *in vitro* passage 2 after differentiation from lesion-derived amastigotes. Intracellular parasite burden was microscopically assessed at 4 h, 48 h and 72 h post-infection (PI) **(Fig. 1A**). We observed a mean number of 8 parasites per macrophage at 4 h PI, which transiently decreased at 48 h but then recovered at 72 h. More than 80% of macrophages were infected at all time points tested (4 h, 48 h and 72 h, data not shown), indicating robust infection and intracellular parasite growth. Infection was similar in both

283 labelled and control macrophages, suggesting that the metabolic labelling did not influence the
284 ability of parasites to survive and proliferate.
285 In a series of control experiments, we assessed the culture system for variations in host cell
286 phenotype, SILAC label incorporation, infection efficiency and protein fractionation technique.
287 Under our experimental conditions (see Materials and Methods), over 90% of the adherent cells
288 differentiated into a homogeneous macrophage population as judged (i) by expression of the
289 macrophage-specific F4/80 surface antigen as determined by fluorescent microscopy [47, 48],
290 and (ii) the ability of the cells to phagocytose fluorescently labeled, yeast zymosan bioparticles
291 (data not shown). We tested the isotope incorporation efficiency in a pilot experiment using
292 Lys4 at day 6 after the differentiation process. Under these conditions, we observed an
293 incorporation rate of "heavy" lysine above 98%, as only 19 proteins out of 1111 proteins were
294 unlabeled. We thus considered that a period of at least six days in SILAC medium is appropriate
295 for performing our proteomics screen (**Fig. 1B**). As shown by the experimental layout in **Fig.**
296 **1C**, we performed label-swap experiments, where the experimental state and stable isotope
297 labels are interchanged. Label swap enriches the list of proteins whose abundance is related to
298 the experimental state as it allows for the identification of systematic errors due to labeling, and
299 to experimental outliers. Bone marrow progenitor cells were differentiated into macrophages
300 in medium supplemented with the 'heavy' amino acid isotopes, referred to as 'labelled" (L),
301 and medium supplemented with the 'light', natural amino acids, referred to as 'control' (C).
302 Cells were infected six days post-differentiation with *L. donovani* promastigotes for 72 h. *L.*
303 *donovani*- infected (I) and non-infected (NI), labeled (L) and control (C) macrophages were
304 lysed, mixed in equal amounts and their proteomes were analysed by LC/MS-MS. Our protocol
305 further included two fractionation methods, SAX and GEL fractionation that are based on
306 charge- or size-dependent separation, respectively. The reduction of extract complexity by these
307 methods is increasing the number of quantifications and thus the quality of our proteomics
308 analyses by increasing protein sequence coverage, which facilitates detection of low-abundance
309 proteins. For these analyses, we performed two label swap experiments and two technical
310 replicates.

311

312 *Analysis and validation of proteomics data*

313 The comparative analysis of macrophage proteomes from reciprocal L-I/ C-NI and C-I/L-NI
314 samples allowed the identification of 5322 and 5101 proteins using SAX and GEL
315 fractionation, respectively and a combined total 6189 proteins (**Fig. 2A** and **Fig. 2B, Table**
316 **S2**). Seventy five percent of proteins identified by GEL and SAX fractionation (3871and 4026
317 proteins, respectively) were shared between L-I/C-NI and C-I /L-NI (**Fig. 2A**), indicating a very
318 good, qualitative reproducibility in the depth of our analysis. Moreover, the overlap between
319 SAX and GEL was also significant, with sixty five percent (3291 proteins) of the proteins
320 identified being shared between the two groups (GEL, SAX: L-I/C-NI and GEL, SAX: L-NI/C-
321 I) (**Fig. 2B**). Volcano plots using GEL and SAX fractionation revealed that a subset of proteins
322 were differentially expressed between in L-I/C-NI and C-I/L-NI (**Fig. 2C**).

323 Amongst the proteins with modulated abundance, only macrophage proteins identified
324 in reciprocal (label swapped) experiments that conformed to raised filtering criteria were
325 selected. To this end, we considered in both forward and reverse experiments a fold change
326 (FC) of 1.25 or higher, with at least 2 peptides identified per quantification. With the exception
327 of "infinite quantifications" – i.e "quantifications" where the proteins were identified in only
328 one of the two compared conditions - only quantifications with confidence level of 0.05 or
329 below ($p \leq 0.05$) in at least one of the experiments were accepted (**Table 1** and **Table 2**).

330 This analysis revealed increased abundance in infected macrophages for 35 proteins
331 (27 proteins with GEL, 8 proteins with SAX), with Glutathione S Transferase mu1
332 (Gstm1/P10649) common in the datasets (**Table 1**). The same analysis revealed reduced
333 abundance for 51 proteins in infected macrophages (42 proteins with GEL, 13 proteins with
334 SAX), with 4 proteins common in the two datasets [the macrophage-expressed gene 1 protein
335 (Mpeg-1/A1L314), Palmitoyl-protein thioesterase 1 (Ppt1/O88531), Cathespin D (Ctsd/
336 P18242) and the Mannose receptor C-type 1 (Mrc-1/Q61830)] (**Table 2**). Thus, for the primary
337 macrophage proteome, these results indicate that SAX and GEL fractionation procedures
338 together increase the level of quantifications that pass the filtering criteria, increasing the depth

of protein quantification. Moreover these data were run against an *L. donovani* database. This analysis revealed that the number of parasite proteins identified ranged between 763 and 1580 (**Table S3**) and a combined total of 1741 proteins (**Table S4**). 55 proteins were shared in each of the quantification between the mouse and the parasitic proteome (**Table S5** and **Table S6**). Comparing these proteins to the proteins listed in **Tables 1** and **2**, only one protein shared one common peptide between mouse and *L. donovani*, namely the 26S protease regulatory subunit (Psmc3/O88685) (**Table 1, Table S5** and **Table S6**), showing that most of the peptides and proteins identified as differentially expressed in this screen are mouse proteins, as 1741 proteins are parasite proteins.

We then validated our results by immunoblot analysis of infected and non-infected macrophages using β-αctin for normalisation. We confirmed reduced abundance in response to infection for Acid ceramidase 1 (Asah1/Q9WV54), Guanine nucleotide exchange factor for Rab-3A (Rab3IL1, Q8TBN0), Heme oxygenase 1 (Hmox-1/P14901) and Cathepsin D (Ctsd /P18242). Additionally, we confirmed the higher abundance of Glutathione S-transferase Mu 1 (Gstm1/P10649) and Plexin A1 (PlxnA1/P70206) (**Fig. 3A**, **Table 1** and **Table 2**). Total RNA of replica samples used for immunoblot analysis was extracted, and reverse transcription (RT) qPCR was performed for selected transcripts. The transcripts of 60S ribosomal protein L19 (RpL19/P84099) and 14-3-3 protein zeta/delta (Ywhaz/P63101) were used as normalisation controls, as these reference genes are considered to have stable expression [49, 50] in these culture conditions. Certain changes in transcript levels correlated with changes in protein abundance, including reduced abundance for Pppt1 and increased abundance for PlxnA1 and the copper-transporting ATPase 1 (Atp7/Q64430). Other transcripts did not show any correlation, e.g., Ctsd, Rab3IL1 and Hmox-1 mRNAs (**Fig. 3B**). These data suggest that *L. donovani* both affects transcriptional and post-transcriptional regulation of infected BMDMs.

Gene Ontology analysis illuminates the landscape of subverted pathways in L. donovani *infected macrophages*

The datasets of differentially modulated proteins were analysed for enriched biological processes, molecular functions and cellular components using the Gene Ontology (GO) and the *Mus musculus* Uniprot databases (https://www.uniprot.org/proteomes/UP000000589), and results were visualised with the BinGO plug-in of the Cytoscape 3.5.1 software package [45]. Up-regulated biological processes were related to metabolism, including lipopolysaccharide biosynthetic process (GO-ID: 9103), cellular ketone metabolic process (GO-ID: 42180), oxoacid (GO-ID: 43436) and carboxylic acid (GO-ID: 19752) metabolism (**Fig. 4A**, **Table S7**), the latter enrichment having previously been observed in THP-1 cells infected with *L. donovani* promastigotes [30]. Enrichment was also observed for various molecular functions, including intramolecular oxidoreductase activity transposing S-S bonds (GO-ID: 16864), intramolecular oxidoreductase activity, interconverting keto and enol groups (GO-ID: 16862) and protein disulfide isomerase activity (GO-ID: 3756)(**Fig. 4B, Table S7**). This last activity is important for protein folding, stress response (balancing the effects of oxidative stress) and phagocytosis [51]. Moreover, enrichment in cellular components included the cytoplasm (GO-ID: 5737), intracellular membrane bounded organelle (GO-ID: 43231) and endoplasmic reticulum (GO-ID: 5783), with many of the up-regulated endoplasmic reticulum (ER) proteins involved in protein folding and post-translation modification (**Fig. 4C**, **Table S7**), revealing a potential impact of *L. donovani* infection on endoplasmic reticulum stress and the unfolded protein response as previously documented [52].

Using the data set of proteins showing reduced abundance, enrichment was observed for biological processes involved in vacuole (GO-ID: 7033) and lysosome (GO-ID: 7040) organisation and catabolic process (GO-ID: 9056) (**Fig. 5A, Table S8**). Enriched molecular functions in the down-modulated dataset, included binding (GO-ID-5488), transcription elongation regulator activity (GO-ID: 3711), hydrolase activity hydrolysing o-glycosyl compounds (GO-ID: 4553) and cysteine type endopeptidase activity enriched in cysteine type endopeptidases (GO-ID: 4197) (**Fig. 5B, Table S8**). Moreover, amongst the enriched cellular components were lytic vacuole (GO-ID: 323), lysosome (GO-ID: 5764) and vacuole (GO-ID: 5773), and thus the very organelles and structures exploited by the parasite as intracellular

394 niche. Other enriched cellular components included cytoplasm (GO-ID: 5737), intracellular
395 membrane bounded organelle, (GO-ID: 43231) and integrin complex (GO-ID: 43231) (**Fig. 5C,**
396 **Table S8)**. .
397
398 L. donovani *modulate the abundance of proteins involved in the lysosome and lytic vacuole*
399 *organisation of BMDMs*
400 Our study reveals that *L. donovani* promastigote infection has a profound effect on BMDM
401 lysosomal biology, with remodeling of this organelle likely promoting parasite survival in its
402 known intracellular niche, the phago-lysosome [4, 53]. Our data show that the ratios of a total
403 of 15 lysosomal proteins in both forward [L-I/C-NI, ratio 1, (r1)] and reverse experiments [C-
404 I/L-NI, ratio 2, (r2)] were below 0.8 (**Table 2** and **Table S7**). Down-regulated proteins included
405 various hydrolases such as lysosomal cathepsins (Ctsb/P10605, r_1 =0.59 r_2=0.54; Ctsc/P97821,
406 r_1=0.49, r_2=0.41; Ctsd/P18242, r_1=0.35, r_2=0.59) or dipeptyl peptidase 2 (Dpp-2/Q9ET22,
407 r_1=0.4, r_2=0.75) and the Lysosome-associated membrane glycoproteins, Lamp2
408 (Cd107b/P17047, r_1=0.72, r_2=0.7) and Lamp4 (Cd68/P31996, r_1=0.68, r_2=0.49) (**Table 2**).
409 Lysosomal proteases, including cathepsins may affect parasite survival as they carry
410 microbicidal activity and are key regulators of the host immune response by modulating Major
411 histocompatibility Class (MHC) II antigen presentation and the trafficking of Toll like receptors
412 (TLRs) [54]. Down-modulation of different cathepsins may cause distinct effects on
413 macrophage activation. For example, deletion or pharmacological inhibition of Ctsb results in
414 inflammatory phenotypes [55, 56] and Ctsd inhibition blocks both Th1 and Th2 responses by
415 strongly suppressing MHCII-associated invariant chain molecule [56]. Different *Leishmania*
416 species and strains, parasite stages (promastigotes/amastigotes) and host species may modulate
417 cathepsins in different ways. For example, Prina *et al* reported a time-dependent increase of
418 Ctsb, Ctsh and Ctsd activity in rat bone marrow-derived macrophages infected with *L.*
419 *amazonensis* [57]. On the other hand, the RNA transcripts of Ctsc and Ctss were reported to be
420 down-modulated in monocyte derived human macrophages 24 h after *L. major* metacyclic
421 promastigote infection [58].

Apart from lysosomal peptidases, a number of hydrolases involved in fatty acid metabolism were also affected in macrophages by *L. donovani* infection. Interestingly, the down-modulation of the lyase Palmitoyl-protein thioesterase 1 (Ppt1/O88531, r_1=0.23, r_2=0.3) involved in the removal of thioester-linked fatty acyl groups (like palmitate) is anticipated to disrupt lysosomal catabolism via the rapid accumulation of palmitoylated proteins [59]. Moreover, Ppt1 down-modulation impairs mTOR signaling [59] the repression of which has been also linked to *Leishmania* intracellular survival [60]. Additionally, down-modulation of Acid ceramidase -1 (Asah-1/Q9WV54, r_1= 0.45, r_2=0.5) (**Table 2**) - an enzyme that hydrolyses the sphingolipid ceramide into sphingosine and free fatty acid - may also impact the macrophage environment to favor parasite survival. *Leishmania* is favored by increase in ceramide concentration and in turn *Leishmania* infection, modulates the up-regulation of ceramide synthesis in a biphasic way [61]. At early time points after *Leishmania* infection, increase is mediated by Acid Sphingomyelinase activation, which catalyses the formation of ceramide from sphingomyelin, promoting the formation of cholesterol rich lipid microdomains [61], required for *L. donovani* uptake by macrophages [62]. In the second phase, the *de novo* biosynthesis of ceramide is induced via ceramide synthase, resulting in the displacement of cholesterol from the membrane and impacting MHC-II class antigen presentation [61]. Moreover, ceramide increase leads to severe host immune suppression via the reduction of nuclear translocation of NFkB and AP-1, the up-regulation of immunosuppressive cytokines TGF-β and IL-10, and reduced NO generation [63]. Thus increase in ceramide concentration is required for parasite survival, and the down-modulation of Asah-1 revealed in this screen, could be an additional mechanism contributing to this rise, and hence merits further investigation.

Interestingly, Fernandes *et al*, have demonstrated that the lysosome is one of the enriched "down-modulated" KEGG pathways in the transcriptome of murine and human macrophages infected with *L. major* [8]. Thus, these results suggest that more than one species of *Leishmania* induce major modifications of lysosomal components, that might aid the parasite to survive inside the hostile macrophage environment. The mechanism that contributes to lysosomal protein down-modulation after *L. donovani* infection, is elusive. One possible

scenario would be a dysregulation of transcription factor EB, which is a master regulator of lysosomal biogenesis that mediates the transcription of many lysosomal hydrolases [64]. Another scenario would be that the lysosomal content is modified via the action of lysosomal exocytosis, which takes place to repair host cell plasma wounding caused by the parasite [65] or by the direct interaction of the parasites' exo-proteases with lysosomal proteins, leading to protein degradation.

L. donovani *induce alterations in abundance of macrophage proteins involved in immunomodulation*

Our data demonstrate that *L. donovani* promastigotes inhibit host cell immune functions by down-regulation of several macrophage proteins that participate in immunomodulation and innate immunity (Cd180/Q62192, r_1=0.66, r_2=0.76; Tlr13/Q6R5N8, r_1=0.66, r_2=0.5; Grn/P28798, r_1=0.7, r_2=0.62; Arrb2/Q91YI4, r_1=0.61, r_2=0.4; Gpr84/Q8CIM5, r_1=0.64 and r_2=1/∞; Hmox-1/P14901, r_1=0.67, r_2=0.39; Mpeg1/A1L314, r_1=0.31, r_2=0.4) (**Table 2**). These results indicate that infection likely dampens the macrophage pro-inflammatory response given the observed down-modulation of (i) Tlr13, which acts via Myd88 and Traf6 leading to NF-κB activation [66], (ii) Granulin (Grn) a soluble cofactor for Tlr9 signaling [67], and (iii) the G-protein coupled receptor Grp84 known to be activated by medium-chain free fatty acids to enhance inflammation and phagocytosis in macrophages [68].

Moreover, *L. donovani* promastigote infection results in increased abundance of macrophage proteins that act as markers or as regulators of alternatively activated macrophages (M2-like phenotype) (**Table 1**) in agreement with previous reports [69-74]. Amongst these proteins were: (i) the Cd9 antigen (P40240, r_1=1.41, r_2=1.76), a tetraspanin family member known to form a complex with integrins and to negatively regulate LPS-induced macrophage activation [75], (ii) the highly up-regulated urokinase-type plasminogen activator (Plau/P06869, r_1=6.02, r_2=5.41) known to polarise macrophages towards a M2-like phenotype [76], (iii) the monoamine oxidase A (Mao-A/Q64133, r_1=1.31, r_2=2.24) involved in the breakdown of monoamines [77], (iv) the TNF alpha induced protein 8 like 2

(Tnfaip8l2/Q9D8Y7, $r_1 = \infty$ and r_2=1.4) involved in phospholipid metabolism [78, 79], (v) the Cd93 antigen (Cd93/O89103, r_1=1.35, r_2=1.76), a C-type lectin transmembrane receptor [80] and (vi) the fatty acid-binding protein (Fabp4/P04117, r_1=1.3, r_2=1.57) that delivers long-chain fatty acids and retinoic acid to their cognate receptors in the nucleus [81] (**Table 1**). Interestingly, Fabp4 up-modulation in infected macrophages is in line with other studies after macrophage infection with *L. major* promastigotes [26] and *L. amazonensis* amastigotes [24], and suggest that the increased abundance of this protein maybe independent of the *Leishmania* stage or species.

In contrast to proteins that control, or are enriched in alternatively activated macrophages, two proteins less abundant in infected macrophages, Cd180 and Beta-arrestin-2 (Arrb2), are known to either promote or reduce inflammation depending on the cell type and infection system [82-85]. Moreover a protein known to be enhanced in alternatively activated macrophages, Hmox-1 that converts pro-oxidant heme to the antioxidant biliverdin and bilirubin, restoring the redox environment [86] was found down-modulated in this screen in response to *Leishmania* infection (**Table 2**). Other studies have shown that Hmox-1 is up-regulated in mouse peritoneal macrophages infected with *L. infantum (L. chagasi*) promastigotes and promotes the persistence of the parasite [87]. In our infection system, despite the repressed protein levels, we find Hmox-1 mRNA to be up-regulated in macrophages infected with *L. donovani*. The negative correlation between Hmox-1 RNA and protein levels, amongst other factors, could be due to increased secretion of Hmox-1 in the culture medium, as Hmox-1 can be a secreted protein [88].

Interestingly, a recent study of Negrão *et al*, which used a label free proteomics approach of the mouse J774 cell line infected with *L. major*, *L. amazonensis* and *L. infantum* promastigotes, 24 h post infection, revealed that certain modulated proteins were also found to be modulated in this study [29]. In the screen of Negrão *et al* proteins with both inverse but also similar regulation to those identified in our screen, were demonstrated. Arrb2 (*L. major*), B2m (*L. amazonensis*) and Hmox-1 (*L. infantum*, *L amazonensis* and *L. major*) were more abundant in the screen of Negrão *et al* [29], in contrast the lower abundance of these proteins in this

report. Proteins with similar regulation include the less abundant Cd180 (*L. infantum*) and Grn (*L. infantum*) [29]. Overall the study of Negrão and colleagues, showed that many up-regulated proteins were involved in the activation of phagocytes and leukocytes, whereas in this screen the differential abundance of many proteins, is anticipated to dampen inflammation, as mentioned above. These differences, could reflect the time of analysis (24 h for Negrão *et al* versus 72 h for this study), as at earlier time points, it is believed that macrophages are generally polarised to a M1 phenotype and at later time points, pathogens subvert macrophage function to a M2 like macrophage, for ensuring survival [7]. Differences could also reflect the *Leishmania* species or the cell type.

L. donovani *up-modulate the abundance of proteins involved in the defense against oxidative and ER stress in BMDMs*

Proteins related to oxidative stress and ER stress response were more abundant in BMDMs 72 h after *L. donovani* infection, including proteins involved in glutathione metabolism, such as Glutamate-cysteine ligase regulatory subunit (Gclm/O09172, r_1=1.28, r_2=1.29), the Glutathione transferase mu1 (Gstm1/P10649, r_1=1.36; r_2=2.53), ferritin light (Ftl1/ P29391, r_1=2.9, r_2=2.64) and heavy (Fth1/P09528, r_1= 1.37, r_2=2.23) chains, and BolA like 1 (Bola1/Q9D8S9, r_1=1.73 and r_2=∞), a protein that prevents mitochondrial changes upon glutathione depletion [89] acting as mitochondrial iron-sulfur cluster assembly factor [90] (**Table 1**). All of these proteins are known to normalise the redox state of the cell or protect the cell from oxidants [89, 91-93]. Interestingly, up-regulated transcripts involved in the response against oxidative stress and glutathione metabolism were previously shown to be up-regulated in human monocyte derived macrophages infected with *L. (Vianna) panamensis* promastigotes [9] and in mouse BMDMs infected with *L. major* promastigotes [26]. Moreover, up rise in cellular ROS, could be associated with ER stress, the unfolded protein (UPR) response and a concomitant up rise of ER proteins aiding protein folding, as a mechanism of the cell to repair oxidant damage [94]. In our system several of these proteins including disulfide-isomerase forms [Protein disulfide-isomerase A3 (Pdia3/ P27773, r_1=1.39,r_2=1.27), A4 (Pdia4/P08003, r_1=1.35, r_2=1.27) and A6

(Pdia6/Q922R8, r_1=1.43 r_2=1.31)] [95] and Hypoxia up-regulated 1 (Hyou1/Q9JKR6, r_1= 1.86, r_2=1.38 [96], displayed higher levels in infected macrophages (**Table 1**). Likewise, ER stress and induction of the unfolded protein response was previously documented for RAW 264.7 cells infected with *L. amazonensis* [52] and in the proteomic study of Singh et al, who showed in THP-1 macrophages infected with *L. donovani*, an increase in the absolute percentage of up-regulated ER proteins, as infection progressed from 12 h and 24 h to 48 h post-infection [30] . Overall, these results suggest that *L. donovani* infection induces ROS production and ER stress [10, 97], with specific proteins involved in this process displaying higher abundance, and likely acting as a defense mechanism against the oxidants' deleterious effects

L. donovani *modulates the abundance macrophage proteins involved in intracellular trafficking and ion movement*

The abundance of many macrophage proteins involved in intracellular trafficking was modified in *L. donovani* infected BMDMs. Previous studies have shown that *Leishmania* infection impairs intracellular trafficking by modulating small GTPase signal transduction [30]. This form of signaling is important in host/pathogen interactions as it regulates pathways involved in phagocytosis and oxidative burst, vesicle fusion and actin organisation [98, 99]. The deregulation of small GTPase signal transduction, likely alters these macrophage functions, and produces a favorable environment for intracellular parasite infection [30, 100, 101]. Our screening extends previous studies and provides evidence of altered protein expression data in proteins involved in small GTPase signalling, with four proteins showing reduced abundance during infection (Gmip Q6PGG2, r_1=0.79, r_2=0.49; Rgl2/Q61193, r_1=1/∞; r_2=0.35; Arfip2/Q8K221, r_1=1/∞ r_2=0.64; Rab3il1/Q8VDV3, r_1=0.66, r_2=0.39; Nisch/Q80TM9, r_1= 0.66, r_2=0.46) (**Table 2**), and one member showing increased abundance (Tbc1d22a/Q8R5A6, r_1=∞ and r_2=1.89) (**Table 1**). Moreover, various other proteins affecting intracellular trafficking were modulated in response to *L. donovani* promastigote infection, including a signal recognition particle receptor subunit beta (Srprb/P47758; r_1=1.36, r_2=1.25) (**Table 1**) that likely restores trafficking imbalances to the ER [102], and two cytoskeletal organisation proteins

562 (Peak1/Q69Z38, r_1=0.45, r_2=0.46; Ppp2r5e/Q61151, r_1=1/∞, r_2=0.73) [103, 104]. Additionally,
563 the abundance of macrophage mannose receptor 1 (Mrc-1) - a protein involved in endocytosis
564 and phagocytosis - was down-modulated (Q61830, r_1=0.63, r_2=0.33), in agreement with
565 previous studies performed with mouse peritoneal macrophages infected with *L. donovani*
566 promastigotes [105]. The study of Singh et al, has also shown that transport and vesicular
567 trafficking is modified in *L. donovani* infected THP-1 macrophages [30], and thus the
568 modulation of these proteins merits further investigation, as they could be part of the parasite
569 evasion strategy interfering with vesicular fusion events in the host cell, important for parasite
570 survival.

571 Interestingly, another form of trafficking, ion movement, has been associated with
572 inflammatory response [106-108]. For example, zinc/copper imbalance reflects immune
573 dysregulation in human leishmaniasis [108]. In this study, some proteins involved in ion
574 transport were modulated in infected BMDMs, including (i) Atp1a1 (Q8VDN2, r_1= 1.39;
575 r_2=1.26) a subunit of the sodium potassium ATPase [109](**Table 1**), (ii) stomatin
576 (Stom/P54116, r_1= 0.78, r_2=0.48) (**Table 2**) known to regulate ion channel activity and
577 transmembrane ion transport [110] and (iii) copper-transporting ATPase 1 (ATP7a/P56542,
578 r_1=2.61, r_2=2.66) that regulates copper efflux under conditions of elevated extracellular copper
579 concentration [111] (**Table 1**). Overall, these changes may reflect immune function and their
580 influence on host/pathogen interaction merits further investigation.
581
582 L. donovani *modulate the abundance of extracellular matrix and adhesion proteins in BMDMs*
583 Macrophage adhesion and cell-cell interactions with other immune cells play important roles
584 in health and disease, with co-stimulatory molecules regulating T cell activation or cell
585 migration enabling leukocyte recruitment to sites of inflammation. Our proteomics screen
586 revealed changes in expression of extracellular matrix and adhesion proteins that could explain
587 the reported modified adhesion of infected macrophages to connective tissue [112]. We
588 confirmed down-modulation of the co-stimulatory molecule Itgax (Q9QXH4, r_1=1/∞, -r_2= 0.33)
589 (**Table 2)**. Changes in abundance of the integrin subunit Itgβ5 (O70309, r_1= 0.73 and r_2=0.55)

which acts with Itga5 as a fibronectin receptor, were detected, as well as differences in other adhesion or adhesion signaling molecules (Nisch/Q80TM9, r_1=0.66, r_2=0.56; Plxna1/ P70206, r_1= 1.65, r_2=2.46; Lpxn/Q99N69, r_1= 0.74, r_2=0.65) (**Table 1** and **Table 2**). Thus, our data expand and further emphasise the impact of intracellular *Leishmania* infection on connective tissue remodeling that may modify host adaptive immune responses mediated by infected macrophages [112, 113].

L. donovani *modulate the abundance of macrophage proteins involved in gene expression*

It is well established that *Leishmania* infection modulates macrophage gene expression [21]. In our study, several proteins implicated at different levels of gene expression regulation, showed differential abundance in response to *L. donovani* BMDM infection, including transcriptional, epigenetic or post-transcriptional regulators (Hist4h4/P62806, r_1=1.44, r_2=1.33; Lpxn/Q99N69, r_1= 0.75, r_2=0.65; Ddx42/ Q810A7, r_1=0.74, r_2=0.65; Psmc3/088685, r_1=1.34, r_2=1.25; Supt5h,/O5520, r_1= 0.67; r_2=0.68; Supt6h/Q62383, r_1=0.59, r_2=0.64), proteins that modify RNA (Cmtr1/Q9DBC3, r_1=1.39 and r_2=∞; Dus3L/Q91XI1, r_1= 0.34, r_2=1/∞), as well as translation regulators (eIF-3/Q9QZD9, r_1= 0.77, r_2=0.73; Rps6ka1-Rsk1/P18653, r_1=0.43, r_2=1/∞) (**Table 1** and **Table 2**). The higher abundance of histone H4 (Hist4h4) in infected macrophages is in accordance with previous reports for *L. donovani* infected THP-1 cells [30], whereas up-regulation of histones is anticipated to have a negative effect on gene expression by the modulation of chromatin structure [114]. Moreover, the lower levels of focal adhesion regulator Lpxn [115, 116] and the increased abundance of the 26S proteasome ATPase component, Psmsc3/TBP-1 [117], two proteins that display novel functions and are known to modulate transcription via specific nuclear receptors [118-120]. Thus the modulation of abundance of these proteins in infected macrophages, may affect transcriptional regulation of *Leishmania* infected macrophages. In addition, Psmsc3/TBP-1 regulates the transcription of Class II trans-activator (CIITA), the master regulator of the MHC-II transcription complex and a critical factor for the initiation of the adaptive immune response [121]. In addition, the down-modulation of specific transcriptional elongation factors (Supt5h and Supt6h) [122-124] is

anticipated to contribute to transcriptomic changes in infected macrophages. The down-modulation of the eukaryotic translation initiation factor eIF-3 and of protein S6 kinase alpha 1(Rps6ka1/Rsk1) - a kinase known to stimulate protein synthesis and a key mediator of mTOR function [125] - suggests that protein translation proceeds at lower rates in infected macrophages [125]. Rps6ka1/Rsk1 is known to "connect the stress-induced activation of transcription factors and mitogens to the ribosome" [126]. This connection is mediated by the activation/phosphorylation of c-Fos, IκBα, cAMP-response element-binding protein (CREB) and CREB-binding protein [127], proteins involved in the inflammatory response. Thus, the modulation of this kinase likely participates in the reprogramming of *Leishmania*-infected macrophages to favor intracellular parasite survival.

L. donovani modulate the abundance of macrophage proteins involved in metabolic processes

Previous studies have shown that *Leishmania* parasites exploit host metabolism to survive inside the hostile macrophage environment. It has been demonstrated that, early during *Leishmania* infection, the aerobic glycolysis predominates with inhibition of the TCA cycle [26], whereas at later time points energy metabolism is shifted towards oxidative phosphorylation and TCA cycle [30, 128]. *Leishmania* infection also perturbs lipid metabolism, including sterol biosynthesis and triacylglyceride synthesis in BMDMs [24, 26]. In our screen, the cellular ketone metabolic process (GO-ID: 42180) and oxoacid metabolic process (GO-ID: 43436) - a broad metabolic processes that includes TCA cycle and aminoacid biosynthesis, were modified, with 5 proteins showing increased abundance (Fabp4/P04117, r_1= 1.3, r_2=1.57; Sucla2/Q9Z2I9, r_1=1.27, r_2=1.37; Phyh/O35386, r_1=∞ and r_2=1.25; Cmas/Q99KK2; r_1= 1.27, r_2=1.72; Gclm/O09172, r_1=1.27, r_2=1.28). Indeed, Succinate--CoA ligase [ADP-forming] subunit beta (Sucla2) – an enzyme that couples the hydrolysis of succinyl-CoA to the synthesis of ATP [129] - was one of the TCA cycle proteins shown to be up-regulated in *L. donovani*-infected THP-1 cells [30]. Likewise, Sterol O-acyltransferase 1 (Soat1/Q61263, r_1=1.29, r_2=1.31) - a cholesterol metabolism enzyme known to form cholesteryl esters from cholesterol

645 [130] – displayed higher levels in infected macrophages (**Table 1**). This change could be related
646 to the increase in cholesterol biosynthesis of macrophages infected with *Leishmania* [24, 26].
647 Finally, fatty acid metabolism, including fatty acid elongation (Ppt1/ O88531, r_1= 0.23,
648 r_2=0.3), phospholipases of the ether lipid metabolic process [(Pla2g7/Q60963, r_1= 0.68, r_2=0.35;
649 Plbd2/ Q3TCN2, r_1=0.71, r_2=0.49) and hydrolases of the sphingolipid metabolism (Asah-
650 1/Q9WV54, r_1=0.45, r_2=0.5; Gla/P51569, r_1=0.63, r_2=0.75; Glb1/P23780, r_1=0.55, r_2=0.76),
651 were found to be less abundant in infected macrophages (**Table 2**). Fatty acid metabolism,
652 including sphingolipid metabolism [131] has been shown to be modulated in macrophages
653 infected with *Leishmania* [24, 26, 61] and is likely to play an important function in
654 *Leishmania*/macrophage interaction.
655
656 *L. donovani modulate the abundance of macrophage proteins that regulate glycan and*
657 *glycoside protein post-translational modifications*
658 In addition, proteins regulating protein sugar (glycan and glycoside) post-translational
659 modifications were modulated in *L. donovani* infected macrophages, with decreased levels
660 observed for (i) ribophorin I (RpnI/Q91YQ5, r_1=1.65, r_2=1.28), an essential subunit of the N-
661 oligosaccharyl transferase (OST) complex which catalyses the N-glycosylation of proteins
662 [132] (**Table 1**), and (ii) alpha and beta galactosidases (Gla/P51569, r_1=0.63, r_2=0.75;
663 Glb1/Q91YQ5, r_1=0.55, r_2=0.76). In contrast, increased abundance was observed for cytidine
664 monophospho-N-acetylneuraminic acid synthetase (Cmas/Q99KK2, r_1=1.27, r_2=1.72) that
665 catalyses the activation of N-acetylneuraminic acid (NeuNAc) to cytidine 5'-monophosphate
666 N-acetylneuraminic acid (CMP-NeuNAc) [133], a substrate required by sialyltransferases for
667 the addition of sialic acid to growing oligosaccharide chains. Conceivably, changes in protein
668 glycosylation may affect protein function and alter immune responses and cell adhesion
669 signaling [134, 135] in infected macrophages, that may favor parasite survival.
670
671 *Conclusions*

In conclusion, our analyses establish a novel experimental framework for the quantitative proteomics analysis of *Leishmania* infected primary macrophages. Our results draw a highly complex picture of *Leishmania*/macrophage interaction and highlight the pleiotropic modulation of biological processes and molecular functions in infected BMDMs that likely establish permissive conditions for intracellular parasite survival and chronic infection. The parasite seems to have developed mechanisms to subvert key macrophage functions and trigger changes in host cell metabolism, innate immunity and lysosomal function. Future experimental validation combining systems-level, phenotypic, and functional genetic analyses is required to correlate enrichment/activation or depletion/inhibition of identified host pathways with changes in intracellular *Leishmania* survival.

Data linking

The mass spectrometry proteomics data have been deposited to the ProteomeXchange Consortium via the PRIDE partner repository [136] with the dataset identifier PXD013448 (username: reviewer19892@ebi.ac.uk, password: 5S8FZXVw).

REFERENCES

[1] S.A. Grevelink, E.A. Lerner, Leishmaniasis, J Am Acad Dermatol 34(2 Pt 1) (1996) 257-72.

[2] J. Alvar, I.D. Velez, C. Bern, M. Herrero, P. Desjeux, J. Cano, J. Jannin, M. den Boer, Leishmaniasis worldwide and global estimates of its incidence, PLoS One 7(5) (2012) e35671.

[3] J. van Griensven, E. Diro, Visceral leishmaniasis, Infect Dis Clin North Am 26(2) (2012) 309-22.

[4] K.P. Chang, D.M. Dwyer, Multiplication of a human parasite (*Leishmania donovani*) in phagolysosomes of hamster macrophages in vitro, Science 193(4254) (1976) 678-80.

[5] A.A. Tarique, J. Logan, E. Thomas, P.G. Holt, P.D. Sly, E. Fantino, Phenotypic, functional, and plasticity features of classical and alternatively activated human macrophages, American journal of respiratory cell and molecular biology 53(5) (2015) 676-88.

[6] C.D. Mills, M1 and M2 Macrophages: Oracles of Health and Disease, Critical reviews in immunology 32(6) (2012) 463-88.

[7] C. Atri, F.Z. Guerfali, D. Laouini, Role of Human Macrophage Polarization in Inflammation during Infectious Diseases, International journal of molecular sciences 19(6) (2018).

[8] M.C. Fernandes, L.A. Dillon, A.T. Belew, H.C. Bravo, D.M. Mosser, N.M. El-Sayed, Dual Transcriptome Profiling of *Leishmania*-Infected Human Macrophages Reveals Distinct Reprogramming Signatures, MBio 7(3) (2016).

[9] C. Ramirez, Y. Diaz-Toro, J. Tellez, T.M. Castilho, R. Rojas, N.A. Ettinger, I. Tikhonova, N.D. Alexander, L. Valderrama, J. Hager, M.E. Wilson, A. Lin, H. Zhao, N.G. Saravia, D. McMahon-Pratt, Human macrophage response to *L. (Viannia) panamensis*: microarray evidence for an early inflammatory response, PLoS Negl Trop Dis 6(10) (2012) e1866.

[10] M. Podinovskaia, A. Descoteaux, *Leishmania* and the macrophage: a multifaceted interaction, Future Microbiol 10(1) (2015) 111-29.

[11] I. Contreras, M.A. Gomez, O. Nguyen, M.T. Shio, R.W. McMaster, M. Olivier, *Leishmania*-induced inactivation of the macrophage transcription factor AP-1 is mediated by the parasite metalloprotease GP63, PLoS Pathog 6(10) (2010) e1001148.

[12] A. Isnard, M.T. Shio, M. Olivier, Impact of *Leishmania* metalloprotease GP63 on macrophage signaling, Front Cell Infect Microbiol 2 (2012) 72.

[13] G.F. Spath, L. Epstein, B. Leader, S.M. Singer, H.A. Avila, S.J. Turco, S.M. Beverley, Lipophosphoglycan is a virulence factor distinct from related glycoconjugates in the protozoan parasite *Leishmania major*, Proceedings of the National Academy of Sciences of the United States of America 97(16) (2000) 9258-63.

[14] G.F. Spath, L.A. Garraway, S.J. Turco, S.M. Beverley, The role(s) of lipophosphoglycan (LPG) in the establishment of *Leishmania major* infections in mammalian hosts, Proceedings of the National Academy of Sciences of the United States of America 100(16) (2003) 9536-41.

[15] G.F. Spath, L.F. Lye, H. Segawa, D.L. Sacks, S.J. Turco, S.M. Beverley, Persistence without pathology in phosphoglycan-deficient *Leishmania major*, Science 301(5637) (2003) 1241-3.

728 [16] N. Moradin, A. Descoteaux, *Leishmania* promastigotes: building a safe niche within
729 macrophages, Front Cell Infect Microbiol 2 (2012) 121.
730 [17] M.E. Winberg, A. Holm, E. Sarndahl, A.F. Vinet, A. Descoteaux, K.E. Magnusson, B.
731 Rasmusson, M. Lerm, *Leishmania donovani* lipophosphoglycan inhibits phagosomal
732 maturation via action on membrane rafts, Microbes Infect 11(2) (2009) 215-22.
733 [18] A.F. Vinet, M. Fukuda, S.J. Turco, A. Descoteaux, The *Leishmania donovani*
734 lipophosphoglycan excludes the vesicular proton-ATPase from phagosomes by impairing the
735 recruitment of synaptotagmin V, PLoS Pathog 5(10) (2009) e1000628.
736 [19] D. Chaussabel, R.T. Semnani, M.A. McDowell, D. Sacks, A. Sher, T.B. Nutman, Unique
737 gene expression profiles of human macrophages and dendritic cells to phylogenetically distinct
738 parasites, Blood 102(2) (2003) 672-81.
739 [20] J.P. Menezes, T.F. Almeida, A.L. Petersen, C.E. Guedes, M.S. Mota, J.G. Lima, L.C.
740 Palma, G.A. Buck, M.A. Krieger, C.M. Probst, P.S. Veras, Proteomic analysis reveals
741 differentially expressed proteins in macrophages infected with *Leishmania amazonensis* or
742 Leishmania major, Microbes Infect 15(8-9) (2013) 579-91.
743 [21] S. Buates, G. Matlashewski, General suppression of macrophage gene expression during
744 *Leishmania donovani* infection, J Immunol 166(5) (2001) 3416-22.
745 [22] L.A. Dillon, R. Suresh, K. Okrah, H. Corrada Bravo, D.M. Mosser, N.M. El-Sayed,
746 Simultaneous transcriptional profiling of *Leishmania major* and its murine macrophage host
747 cell reveals insights into host-pathogen interactions, BMC Genomics 16 (2015) 1108.
748 [23] N.A. Ettinger, M.E. Wilson, Macrophage and T-cell gene expression in a model of early
749 infection with the protozoan *Leishmania chagasi*, PLoS Negl Trop Dis 2(6) (2008) e252.
750 [24] J. Osorio y Fortea, E. de La Llave, B. Regnault, J.Y. Coppee, G. Milon, T. Lang, E. Prina,
751 Transcriptional signatures of BALB/c mouse macrophages housing multiplying *Leishmania*
752 *amazonensis* amastigotes, BMC Genomics 10 (2009) 119.
753 [25] C. Ovalle-Bracho, C. Franco-Munoz, D. Londono-Barbosa, D. Restrepo-Montoya, C.
754 Clavijo-Ramirez, Changes in Macrophage Gene Expression Associated with *Leishmania*
755 *(Viannia) braziliensis* Infection, PLoS One 10(6) (2015) e0128934.

[26] I. Rabhi, S. Rabhi, R. Ben-Othman, A. Rasche, A. Daskalaki, B. Trentin, D. Piquemal, B. Regnault, A. Descoteaux, L. Guizani-Tabbane, C. Sysco, Transcriptomic signature of *Leishmania* infected mice macrophages: a metabolic point of view, PLoS Negl Trop Dis 6(8) (2012) e1763.

[27] N.E. Rodriguez, H.K. Chang, M.E. Wilson, Novel program of macrophage gene expression induced by phagocytosis of *Leishmania chagasi*, Infect Immun 72(4) (2004) 2111-22.

[28] P.S. Veras, J.P. Bezerra de Menezes, Using Proteomics to Understand How *Leishmania* Parasites Survive inside the Host and Establish Infection, International journal of molecular sciences 17(8) (2016).

[29] F. Negrao, C. Fernandez-Costa, N. Zorgi, S. Giorgio, M. Nogueira Eberlin, J.R. Yates, 3rd, Label-Free Proteomic Analysis Reveals Parasite-Specific Protein Alterations in Macrophages Following *Leishmania amazonensis*, *Leishmania major*, or *Leishmania infantum* Infection, ACS infectious diseases 5(6) (2019) 851-862.

[30] A.K. Singh, R.K. Pandey, J.L. Siqueira-Neto, Y.J. Kwon, L.H. Freitas-Junior, C. Shaha, R. Madhubala, Proteomic-based approach to gain insight into reprogramming of THP-1 cells exposed to *Leishmania donovani* over an early temporal window, Infect Immun 83(5) (2015) 1853-68.

[31] H. Bosshart, M. Heinzelmann, THP-1 cells as a model for human monocytes, Annals of translational medicine 4(21) (2016) 438.

[32] W. Chanput, J.J. Mes, H.J. Wichers, THP-1 cell line: an i*n vitro* cell model for immune modulation approach, International immunopharmacology 23(1) (2014) 37-45.

[33] A. Schildberger, E. Rossmanith, T. Eichhorn, K. Strassl, V. Weber, Monocytes, peripheral blood mononuclear cells, and THP-1 cells exhibit different cytokine expression patterns following stimulation with lipopolysaccharide, Mediators of inflammation 2013 (2013) 697972.

782 [34] S. Tsuchiya, M. Yamabe, Y. Yamaguchi, Y. Kobayashi, T. Konno, K. Tada, Establishment
783 and characterization of a human acute monocytic leukemia cell line (THP-1), International
784 journal of cancer 26(2) (1980) 171-6.
785 [35] Z. Li, R.M. Adams, K. Chourey, G.B. Hurst, R.L. Hettich, C. Pan, Systematic comparison
786 of label-free, metabolic labeling, and isobaric chemical labeling for quantitative proteomics on
787 LTQ Orbitrap Velos, Journal of proteome research 11(3) (2012) 1582-90.
788 [36] S.E. Ong, B. Blagoev, I. Kratchmarova, D.B. Kristensen, H. Steen, A. Pandey, M. Mann,
789 Stable isotope labeling by amino acids in cell culture, SILAC, as a simple and accurate approach
790 to expression proteomics, Molecular & cellular proteomics : MCP 1(5) (2002) 376-86.
791 [37] P. Pescher, T. Blisnick, P. Bastin, G.F. Spath, Quantitative proteome profiling informs on
792 phenotypic traits that adapt *Leishmania donovani* for axenic and intracellular proliferation, Cell
793 Microbiol 13(7) (2011) 978-91.
794 [38] J.R. Wisniewski, A. Zougman, M. Mann, Combination of FASP and StageTip-based
795 fractionation allows in-depth analysis of the hippocampal membrane proteome, Journal of
796 proteome research 8(12) (2009) 5674-8.
797 [39] P. Poullet, S. Carpentier, E. Barillot, myProMS, a web server for management and
798 validation of mass spectrometry-based proteomic data, Proteomics 7(15) (2007) 2553-6.
799 [40] M.E. Ritchie, B. Phipson, D. Wu, Y. Hu, C.W. Law, W. Shi, G.K. Smyth, limma powers
800 differential expression analyses for RNA-sequencing and microarray studies, Nucleic Acids
801 Res 43(7) (2015) e47.
802 [41] Y. Benjamini, H. Y., Controlling the False Discovery Rate: A Practical and Powerful
803 Approach to Multiple Testing Journal of the Royal Statistical Society. Series B
804 (Methodological) 57(1) (2015) 289-300.
805 [42] J. Hellemans, G. Mortier, A. De Paepe, F. Speleman, J. Vandesompele, qBase relative
806 quantification framework and software for management and automated analysis of real-time
807 quantitative PCR data, Genome biology 8(2) (2007) R19.

[43] E. Prina, E. Roux, D. Mattei, G. Milon, Leishmania DNA is rapidly degraded following parasite death: an analysis by microscopy and real-time PCR, Microbes Infect 9(11) (2007) 1307-15.

[44] D. Smirlis, H. Boleti, M. Gaitanou, M. Soto, K. Soteriadou, *Leishmania donovani* Ran-GTPase interacts at the nuclear rim with linker histone H1, The Biochemical journal 424(3) (2009) 367-74.

[45] P. Shannon, A. Markiel, O. Ozier, N.S. Baliga, J.T. Wang, D. Ramage, N. Amin, B. Schwikowski, T. Ideker, Cytoscape: a software environment for integrated models of biomolecular interaction networks, Genome research 13(11) (2003) 2498-504.

[46] S. Maere, K. Heymans, M. Kuiper, BiNGO: a Cytoscape plugin to assess overrepresentation of gene ontology categories in biological networks, Bioinformatics 21(16) (2005) 3448-9.

[47] J.M. Austyn, S. Gordon, F4/80, a monoclonal antibody directed specifically against the mouse macrophage, Eur J Immunol 11(10) (1981) 805-15.

[48] I.D. Haidl, W.A. Jefferies, The macrophage cell surface glycoprotein F4/80 is a highly glycosylated proteoglycan, Eur J Immunol 26(5) (1996) 1139-46.

[49] M.R. Facci, G. Auray, F. Meurens, R. Buchanan, J. van Kessel, V. Gerdts, Stability of expression of reference genes in porcine peripheral blood mononuclear and dendritic cells, Veterinary immunology and immunopathology 141(1-2) (2011) 11-5.

[50] C.S. Thiel, S. Hauschild, S. Tauber, K. Paulsen, C. Raig, A. Raem, J. Biskup, A. Gutewort, E. Hurlimann, F. Unverdorben, I. Buttron, B. Lauber, C. Philpot, H. Lier, F. Engelmann, L.E. Layer, O. Ullrich, Identification of reference genes in human myelomonocytic cells for gene expression studies in altered gravity, Biomed Res Int 2015 (2015) 363575.

[51] C.X. Santos, B.S. Stolf, P.V. Takemoto, A.M. Amanso, L.R. Lopes, E.B. Souza, H. Goto, F.R. Laurindo, Protein disulfide isomerase (PDI) associates with NADPH oxidase and is required for phagocytosis of *Leishmania chagasi* promastigotes by macrophages, Journal of leukocyte biology 86(4) (2009) 989-98.

[52] K.L. Dias-Teixeira, T.C. Calegari-Silva, G.R. dos Santos, J. Vitorino Dos Santos, C. Lima, J.M. Medina, B.H. Aktas, U.G. Lopes, The integrated endoplasmic reticulum stress response in *Leishmania amazonensis* macrophage infection: the role of X-box binding protein 1 transcription factor, FASEB journal : official publication of the Federation of American Societies for Experimental Biology 30(4) (2016) 1557-65.

[53] J. Alexander, K. Vickerman, Fusion of host cell secondary lysosomes with the parasitophorous vacuoles of *Leishmania mexicana*-infected macrophages, The Journal of protozoology 22(4) (1975) 502-8.

[54] S.I. van Kasteren, H.S. Overkleeft, Endo-lysosomal proteases in antigen presentation, Current opinion in chemical biology 23 (2014) 8-15.

[55] I.J. Gonzalez-Leal, B. Roger, A. Schwarz, T. Schirmeister, T. Reinheckel, M.B. Lutz, H. Moll, Cathepsin B in antigen-presenting cells controls mediators of the Th1 immune response during *Leishmania major* infection, PLoS Negl Trop Dis 8(9) (2014) e3194.

[56] T. Zhang, Y. Maekawa, J. Hanba, T. Dainichi, B.F. Nashed, H. Hisaeda, T. Sakai, T. Asao, K. Himeno, R.A. Good, N. Katunuma, Lysosomal cathepsin B plays an important role in antigen processing, while cathepsin D is involved in degradation of the invariant chain inovalbumin-immunized mice, Immunology 100(1) (2000) 13-20.

[57] E. Prina, J.C. Antoine, B. Wiederanders, H. Kirschke, Localization and activity of various lysosomal proteases in *Leishmania amazonensis*-infected macrophages, Infect Immun 58(6) (1990) 1730-7.

[58] F.Z. Guerfali, D. Laouini, L. Guizani-Tabbane, F. Ottones, K. Ben-Aissa, A. Benkahla, L. Manchon, D. Piquemal, S. Smandi, O. Mghirbi, T. Commes, J. Marti, K. Dellagi, Simultaneous gene expression profiling in human macrophages infected with *Leishmania major* parasites using SAGE, BMC Genomics 9 (2008) 238.

[59] V.W. Rebecca, M.C. Nicastri, N. McLaughlin, C. Fennelly, Q. McAfee, A. Ronghe, M. Nofal, C.Y. Lim, E. Witze, C.I. Chude, G. Zhang, G.M. Alicea, S. Piao, S. Murugan, R. Ojha, S.M. Levi, Z. Wei, J.S. Barber-Rotenberg, M.E. Murphy, G.B. Mills, Y. Lu, J. Rabinowitz, R. Marmorstein, Q. Liu, S. Liu, X. Xu, M. Herlyn, R. Zoncu, D.C. Brady, D.W. Speicher, J.D.

863 Winkler, R.K. Amaravadi, A Unified Approach to Targeting the Lysosome's Degradative and
864 Growth Signaling Roles, Cancer discovery 7(11) (2017) 1266-1283.
865 [60] M. Jaramillo, M.A. Gomez, O. Larsson, M.T. Shio, I. Topisirovic, I. Contreras, R.
866 Luxenburg, A. Rosenfeld, R. Colina, R.W. McMaster, M. Olivier, M. Costa-Mattioli, N.
867 Sonenberg, *Leishmania* repression of host translation through mTOR cleavage is required for
868 parasite survival and infection, Cell Host Microbe 9(4) (2011) 331-41.
869 [61] S. Majumder, R. Dey, S. Bhattacharjee, A. Rub, G. Gupta, S. Bhattacharyya Majumdar,
870 B. Saha, S. Majumdar, *Leishmania*-induced biphasic ceramide generation in macrophages is
871 crucial for uptake and survival of the parasite, J Infect Dis 205(10) (2012) 1607-16.
872 [62] T.J. Pucadyil, P. Tewary, R. Madhubala, A. Chattopadhyay, Cholesterol is required for
873 *Leishmania donovani* infection: implications in leishmaniasis, Molecular and biochemical
874 parasitology 133(2) (2004) 145-52.
875 [63] J.J. Jawed, S. Parveen, S. Majumdar, Ceramide in the Establishment of Visceral
876 Leishmaniasis, an Insight into Membrane Architecture and Pathogenicity, in: M. H.K. (Ed.),
877 Molecular Biology of Kinetoplastid Parasites, Caister Academic Press, Kolkata, India, 2018,
878 pp. 111-118.
879 [64] L. Bajaj, P. Lotfi, R. Pal, A.D. Ronza, J. Sharma, M. Sardiello, Lysosome biogenesis in
880 health and disease, Journal of neurochemistry (2018).
881 [65] C.L. Forestier, C. Machu, C. Loussert, P. Pescher, G.F. Spath, Imaging host cell-
882 *Leishmania interaction* dynamics implicates parasite motility, lysosome recruitment, and host
883 cell wounding in the infection process, Cell Host Microbe 9(4) (2011) 319-30.
884 [66] Y. Ren, D. Ding, B. Pan, W. Bu, The TLR13-MyD88-NF-kappaB signalling pathway of
885 Cyclina sinensis plays vital roles in innate immune responses, Fish & shellfish immunology 70
886 (2017) 720-730.
887 [67] B. Park, L. Buti, S. Lee, T. Matsuwaki, E. Spooner, M.M. Brinkmann, M. Nishihara, H.L.
888 Ploegh, Granulin is a soluble cofactor for toll-like receptor 9 signaling, Immunity 34(4) (2011)
889 505-13.

[68] C. Recio, D. Lucy, G.S.D. Purvis, P. Iveson, L. Zeboudj, A.J. Iqbal, D. Lin, C. O'Callaghan, L. Davison, E. Griesbach, A.J. Russell, G.M. Wynne, L. Dib, C. Monaco, D.R. Greaves, Activation of the Immune-Metabolic Receptor GPR84 Enhances Inflammation and Phagocytosis in Macrophages, Frontiers in immunology 9 (2018) 1419.

[69] G. Forget, K.A. Siminovitch, S. Brochu, S. Rivest, D. Radzioch, M. Olivier, Role of host phosphotyrosine phosphatase SHP-1 in the development of murine leishmaniasis, Eur J Immunol 31(11) (2001) 3185-96.

[70] W.C. Kwan, W.R. McMaster, N. Wong, N.E. Reiner, Inhibition of expression of major histocompatibility complex class II molecules in macrophages infected with *Leishmania donovani* occurs at the level of gene transcription via a cyclic AMP-independent mechanism, Infect Immun 60(5) (1992) 2115-20.

[71] D. Nandan, R. Lo, N.E. Reiner, Activation of phosphotyrosine phosphatase activity attenuates mitogen-activated protein kinase signaling and inhibits c-FOS and nitric oxide synthase expression in macrophages infected with Leishmania donovani, Infect Immun 67(8) (1999) 4055-63.

[72] D. Nandan, N.E. Reiner, Attenuation of gamma interferon-induced tyrosine phosphorylation in mononuclear phagocytes infected with *Leishmania donovani*: selective inhibition of signaling through Janus kinases and Stat1, Infect Immun 63(11) (1995) 4495-500.

[73] M. Olivier, R.W. Brownsey, N.E. Reiner, Defective stimulus-response coupling in human monocytes infected with Leishmania donovani is associated with altered activation and translocation of protein kinase C, Proceedings of the National Academy of Sciences of the United States of America 89(16) (1992) 7481-5.

[74] N.E. Reiner, Altered cell signaling and mononuclear phagocyte deactivation during intracellular infection, Immunology today 15(8) (1994) 374-81.

[75] M. Suzuki, I. Tachibana, Y. Takeda, P. He, S. Minami, T. Iwasaki, H. Kida, S. Goya, T. Kijima, M. Yoshida, T. Kumagai, T. Osaki, I. Kawase, Tetraspanin CD9 negatively regulates lipopolysaccharide-induced macrophage activation and lung inflammation, J Immunol 182(10) (2009) 6485-93.

[76] J. Meznarich, L. Malchodi, D. Helterline, S.A. Ramsey, K. Bertko, T. Plummer, A. Plawman, E. Gold, A. Stempien-Otero, Urokinase plasminogen activator induces pro-fibrotic/m2 phenotype in murine cardiac macrophages, PLoS One 8(3) (2013) e57837.

[77] M.K. Cathcart, A. Bhattacharjee, Monoamine oxidase A (MAO-A): a signature marker of alternatively activated monocytes/macrophages, Inflammation and cell signaling 1(4) (2014).

[78] P. Antony, B. Baby, R. Vijayan, Molecular insights into the binding of phosphoinositides to the TH domain region of TIPE proteins, Journal of molecular modeling 22(11) (2016) 272.

[79] H. Sun, S. Gong, R.J. Carmody, A. Hilliard, L. Li, J. Sun, L. Kong, L. Xu, B. Hilliard, S. Hu, H. Shen, X. Yang, Y.H. Chen, TIPE2, a negative regulator of innate and adaptive immunity that maintains immune homeostasis, Cell 133(3) (2008) 415-26.

[80] M. Beyer, M.R. Mallmann, J. Xue, A. Staratschek-Jox, D. Vorholt, W. Krebs, D. Sommer, J. Sander, C. Mertens, A. Nino-Castro, S.V. Schmidt, J.L. Schultze, High-resolution transcriptome of human macrophages, PLoS One 7(9) (2012) e45466.

[81] G.S. Hotamisligil, D.A. Bernlohr, Metabolic functions of FABPs--mechanisms and therapeutic implications, Nature reviews. Endocrinology 11(10) (2015) 592-605.

[82] A. Blumenthal, T. Kobayashi, L.M. Pierini, N. Banaei, J.D. Ernst, K. Miyake, S. Ehrt, RP105 facilitates macrophage activation by *Mycobacterium tuberculosis* lipoproteins, Cell Host Microbe 5(1) (2009) 35-46.

[83] S.M. DeWire, S. Ahn, R.J. Lefkowitz, S.K. Shenoy, Beta-arrestins and cell signaling, Annual review of physiology 69 (2007) 483-510.

[84] T.E. Schultz, A. Blumenthal, The RP105/MD-1 complex: molecular signaling mechanisms and pathophysiological implications, Journal of leukocyte biology 101(1) (2017) 183-192.

[85] C.H. Yu, M. Micaroni, A. Puyskens, T.E. Schultz, J.C. Yeo, A.C. Stanley, M. Lucas, J. Kurihara, K.M. Dobos, J.L. Stow, A. Blumenthal, RP105 Engages Phosphatidylinositol 3-Kinase p110delta To Facilitate the Trafficking and Secretion of Cytokines in Macrophages during Mycobacterial Infection, J Immunol 195(8) (2015) 3890-900.

[86] H.M. Schipper, W. Song, A. Tavitian, M. Cressatti, The sinister face of heme oxygenase-1 in brain aging and disease, Progress in neurobiology (2018).

946 [87] N.F. Luz, B.B. Andrade, D.F. Feijo, T. Araujo-Santos, G.Q. Carvalho, D. Andrade, D.R.
947 Abanades, E.V. Melo, A.M. Silva, C.I. Brodskyn, M. Barral-Netto, A. Barral, R.P. Soares, R.P.
948 Almeida, M.T. Bozza, V.M. Borges, Heme oxygenase-1 promotes the persistence of
949 Leishmania chagasi infection, J Immunol 188(9) (2012) 4460-7.
950 [88] C. Davis, A. Dukes, M. Drewry, I. Helwa, M.H. Johnson, C.M. Isales, W.D. Hill, Y. Liu,
951 X. Shi, S. Fulzele, M.W. Hamrick, MicroRNA-183-5p Increases with Age in Bone-Derived
952 Extracellular Vesicles, Suppresses Bone Marrow Stromal (Stem) Cell Proliferation, and
953 Induces Stem Cell Senescence, Tissue engineering. Part A 23(21-22) (2017) 1231-1240.
954 [89] P. Willems, B.F. Wanschers, J. Esseling, R. Szklarczyk, U. Kudla, I. Duarte, M. Forkink,
955 M. Nooteboom, H. Swarts, J. Gloerich, L. Nijtmans, W. Koopman, M.A. Huynen, BOLA1 is
956 an aerobic protein that prevents mitochondrial morphology changes induced by glutathione
957 depletion, Antioxidants & redox signaling 18(2) (2013) 129-38.
958 [90] M.A. Uzarska, V. Nasta, B.D. Weiler, F. Spantgar, S. Ciofi-Baffoni, M.R. Saviello, L.
959 Gonnelli, U. Muhlenhoff, L. Banci, R. Lill, Mitochondrial Bol1 and Bol3 function as assembly
960 factors for specific iron-sulfur proteins, eLife 5 (2016).
961 [91] Y. Fan, J. Zhang, L. Cai, S. Wang, C. Liu, Y. Zhang, L. You, Y. Fu, Z. Shi, Z. Yin, L. Luo,
962 Y. Chang, X. Duan, The effect of anti-inflammatory properties of ferritin light chain on
963 lipopolysaccharide-induced inflammatory response in murine macrophages, Biochimica et
964 biophysica acta 1843(11) (2014) 2775-83.
965 [92] H. Kimura, Hydrogen sulfide and polysulfides as biological mediators, Molecules 19(10)
966 (2014) 16146-57.
967 [93] K. Kinnula, K. Linnainmaa, K.O. Raivio, V.L. Kinnula, Endogenous antioxidant enzymes
968 and glutathione S-transferase in protection of mesothelioma cells against hydrogen peroxide
969 and epirubicin toxicity, British journal of cancer 77(7) (1998) 1097-102.
970 [94] J.D. Malhotra, R.J. Kaufman, Endoplasmic reticulum stress and oxidative stress: a vicious
971 cycle or a double-edged sword?, Antioxidants & redox signaling 9(12) (2007) 2277-93.

[95] E.R. Perri, C.J. Thomas, S. Parakh, D.M. Spencer, J.D. Atkin, The Unfolded Protein Response and the Role of Protein Disulfide Isomerase in Neurodegeneration, Frontiers in cell and developmental biology 3 (2015) 80.

[96] Y. Kitao, K. Ozawa, M. Miyazaki, M. Tamatani, T. Kobayashi, H. Yanagi, M. Okabe, M. Ikawa, T. Yamashima, D.M. Stern, O. Hori, S. Ogawa, Expression of the endoplasmic reticulum molecular chaperone (ORP150) rescues hippocampal neurons from glutamate toxicity, J Clin Invest 108(10) (2001) 1439-50.

[97] L. Galluzzi, A. Diotallevi, M. Magnani, Endoplasmic reticulum stress and unfolded protein response in infection by intracellular parasites, Future science OA 3(3) (2017) FSO198.

[98] K. Bedard, K.H. Krause, The NOX family of ROS-generating NADPH oxidases: physiology and pathophysiology, Physiological reviews 87(1) (2007) 245-313.

[99] J.H. Exton, Small GTPases minireview series, J Biol Chem 273(32) (1998) 19923.

[100] J.L. Johnson, J. Monfregola, G. Napolitano, W.B. Kiosses, S.D. Catz, Vesicular trafficking through cortical actin during exocytosis is regulated by the Rab27a effector JFC1/Slp1 and the RhoA-GTPase-activating protein Gem-interacting protein, Molecular biology of the cell 23(10) (2012) 1902-16.

[101] J. Peranen, Rab8 GTPase as a regulator of cell shape, Cytoskeleton 68(10) (2011) 527-39.

[102] M. Hortsch, D. Avossa, D.I. Meyer, Characterization of secretory protein translocation: ribosome-membrane interaction in endoplasmic reticulum, The Journal of cell biology 103(1) (1986) 241-53.

[103] T. Hyodo, S. Ito, E. Asano-Inami, D. Chen, T. Senga, A regulatory subunit of protein phosphatase 2A, PPP2R5E, regulates the abundance of microtubule crosslinking factor 1, The FEBS journal 283(19) (2016) 3662-3671.

[104] Y. Wang, J.A. Kelber, H.S. Tran Cao, G.T. Cantin, R. Lin, W. Wang, S. Kaushal, J.M. Bristow, T.S. Edgington, R.M. Hoffman, M. Bouvet, J.R. Yates, 3rd, R.L. Klemke, Pseudopodium-enriched atypical kinase 1 regulates the cytoskeleton and cancer progression

999 [corrected], Proceedings of the National Academy of Sciences of the United States of America
1000 107(24) (2010) 10920-5.
1001 [105] N. Basu, R. Sett, P.K. Das, Down-regulation of mannose receptors on macrophages after
1002 infection with Leishmania donovani, The Biochemical journal 277 (Pt 2) (1991) 451-6.
1003 [106] K.Y. Djoko, C.L. Ong, M.J. Walker, A.G. McEwan, The Role of Copper and Zinc
1004 Toxicity in Innate Immune Defense against Bacterial Pathogens, J Biol Chem 290(31) (2015)
1005 18954-61.
1006 [107] S. Hojyo, T. Fukada, Roles of Zinc Signaling in the Immune System, Journal of
1007 immunology research 2016 (2016) 6762343.
1008 [108] J. Van Weyenbergh, G. Santana, A. D'Oliveira, Jr., A.F. Santos, Jr., C.H. Costa, E.M.
1009 Carvalho, A. Barral, M. Barral-Netto, Zinc/copper imbalance reflects immune dysfunction in
1010 human leishmaniasis: an ex vivo and in vitro study, BMC infectious diseases 4 (2004) 50.
1011 [109] J.T. Chang, L.A. Lowery, H. Sive, Multiple roles for the Na,K-ATPase subunits, Atp1a1
1012 and Fxyd1, during brain ventricle development, Developmental biology 368(2) (2012) 312-22.
1013 [110] M.P. Price, R.J. Thompson, J.O. Eshcol, J.A. Wemmie, C.J. Benson, Stomatin modulates
1014 gating of acid-sensing ion channels, J Biol Chem 279(51) (2004) 53886-91.
1015 [111] S. Lutsenko, A. Gupta, J.L. Burkhead, V. Zuzel, Cellular multitasking: the dual role of
1016 human Cu-ATPases in cofactor delivery and intracellular copper balance, Archives of
1017 biochemistry and biophysics 476(1) (2008) 22-32.
1018 [112] C.P. Figueira, D.G. Carvalhal, R.A. Almeida, M. Hermida, D. Touchard, P. Robert, A.
1019 Pierres, P. Bongrand, W.L. dos-Santos, *Leishmania* infection modulates beta-1 integrin
1020 activation and alters the kinetics of monocyte spreading over fibronectin, Scientific reports 5
1021 (2015) 12862.
1022 [113] S.S. Costa, M.C. Fornazim, A.E. Nowill, S. Giorgio, *Leishmania amazonensis* induces
1023 modulation of costimulatory and surface marker molecules in human macrophages, Parasite
1024 immunology 40(4) (2018) e12519.
1025 [114] J. Svaren, W. Horz, Histones, nucleosomes and transcription, Current opinion in genetics
1026 & development 3(2) (1993) 219-25.

[115] P.W. Chen, G.S. Kroog, Leupaxin is similar to paxillin in focal adhesion targeting and tyrosine phosphorylation but has distinct roles in cell adhesion and spreading, Cell adhesion & migration 4(4) (2010) 527-40.

[116] T. Tanaka, K. Moriwaki, S. Murata, M. Miyasaka, LIM domain-containing adaptor, leupaxin, localizes in focal adhesion and suppresses the integrin-induced tyrosine phosphorylation of paxillin, Cancer science 101(2) (2010) 363-8.

[117] G.C. Lander, E. Estrin, M.E. Matyskiela, C. Bashore, E. Nogales, A. Martin, Complete subunit architecture of the proteasome regulatory particle, Nature 482(7384) (2012) 186-91.

[118] S. Kaulfuss, M. Grzmil, B. Hemmerlein, P. Thelen, S. Schweyer, J. Neesen, L. Bubendorf, A.G. Glass, H. Jarry, B. Auber, P. Burfeind, Leupaxin, a novel coactivator of the androgen receptor, is expressed in prostate cancer and plays a role in adhesion and invasion of prostate carcinoma cells, Molecular endocrinology 22(7) (2008) 1606-21.

[119] S. Kaulfuss, A.M. Herr, A. Buchner, B. Hemmerlein, A.R. Gunthert, P. Burfeind, Leupaxin is expressed in mammary carcinoma and acts as a transcriptional activator of the estrogen receptor alpha, International journal of oncology 47(1) (2015) 106-14.

[120] T. Satoh, T. Ishizuka, T. Tomaru, S. Yoshino, Y. Nakajima, K. Hashimoto, N. Shibusawa, T. Monden, M. Yamada, M. Mori, Tat-binding protein-1 (TBP-1), an ATPase of 19S regulatory particles of the 26S proteasome, enhances androgen receptor function in cooperation with TBP-1-interacting protein/Hop2, Endocrinology 150(7) (2009) 3283-90.

[121] A.D. Truax, O.I. Koues, M.K. Mentel, S.F. Greer, The 19S ATPase S6a (S6'/TBP1) regulates the transcription initiation of class II transactivator, Journal of molecular biology 395(2) (2010) 254-69.

[122] M. Endoh, W. Zhu, J. Hasegawa, H. Watanabe, D.K. Kim, M. Aida, N. Inukai, T. Narita, T. Yamada, A. Furuya, H. Sato, Y. Yamaguchi, S.S. Mandal, D. Reinberg, T. Wada, H. Handa, Human Spt6 stimulates transcription elongation by RNA polymerase II in vitro, Molecular and cellular biology 24(8) (2004) 3324-36.

[123] B. Stadelmayer, G. Micas, A. Gamot, P. Martin, N. Malirat, S. Koval, R. Raffel, B. Sobhian, D. Severac, S. Rialle, H. Parrinello, O. Cuvier, M. Benkirane, Integrator complex

regulates NELF-mediated RNA polymerase II pause/release and processivity at coding genes, Nature communications 5 (2014) 5531.

[124] T. Wada, T. Takagi, Y. Yamaguchi, A. Ferdous, T. Imai, S. Hirose, S. Sugimoto, K. Yano, G.A. Hartzog, F. Winston, S. Buratowski, H. Handa, DSIF, a novel transcription elongation factor that regulates RNA polymerase II processivity, is composed of human Spt4 and Spt5 homologs, Genes & development 12(3) (1998) 343-56.

[125] K. Jastrzebski, K.M. Hannan, E.B. Tchoubrieva, R.D. Hannan, R.B. Pearson, Coordinate regulation of ribosome biogenesis and function by the ribosomal protein S6 kinase, a key mediator of mTOR function, Growth factors 25(4) (2007) 209-26.

[126] T.R. Peterson, D.M. Sabatini, eIF3: a connecTOR of S6K1 to the translation preinitiation complex, Molecular cell 20(5) (2005) 655-7.

[127] M. Frodin, S. Gammeltoft, Role and regulation of 90 kDa ribosomal S6 kinase (RSK) in signal transduction, Molecular and cellular endocrinology 151(1-2) (1999) 65-77.

[128] D. Moreira, V. Rodrigues, M. Abengozar, L. Rivas, E. Rial, M. Laforge, X. Li, M. Foretz, B. Viollet, J. Estaquier, A. Cordeiro da Silva, R. Silvestre, Leishmania infantum modulates host macrophage mitochondrial metabolism by hijacking the SIRT1-AMPK axis, PLoS Pathog 11(3) (2015) e1004684.

[129] O. Elpeleg, C. Miller, E. Hershkovitz, M. Bitner-Glindzicz, G. Bondi-Rubinstein, S. Rahman, A. Pagnamenta, S. Eshhar, A. Saada, Deficiency of the ADP-forming succinyl-CoA synthase activity is associated with encephalomyopathy and mitochondrial DNA depletion, American journal of human genetics 76(6) (2005) 1081-6.

[130] K.M. Cadigan, J.G. Heider, T.Y. Chang, Isolation and characterization of Chinese hamster ovary cell mutants deficient in acyl-coenzyme A:cholesterol acyltransferase activity, J Biol Chem 263(1) (1988) 274-82.

[131] S. Grosch, A.V. Alessenko, E. Albi, The Many Facets of Sphingolipids in the Specific Phases of Acute Inflammatory Response, Mediators of inflammation 2018 (2018) 5378284.

[132] C.M. Wilson, Q. Roebuck, S. High, Ribophorin I regulates substrate delivery to the oligosaccharyltransferase core, Proceedings of the National Academy of Sciences of the United States of America 105(28) (2008) 9534-9.

[133] W. van Wijk, W. Ferwerda, D.H. van den Eijnden, Cytidine 5'-monophospho-N-acetylneuraminic acid synthetase of calf kidney, Hoppe-Seyler's Zeitschrift fur physiologische Chemie 353(10) (1972) 1507-8.

[134] E. Maverakis, K. Kim, M. Shimoda, M.E. Gershwin, F. Patel, R. Wilken, S. Raychaudhuri, L.R. Ruhaak, C.B. Lebrilla, Glycans in the immune system and The Altered Glycan Theory of Autoimmunity: a critical review, Journal of autoimmunity 57 (2015) 1-13.

[135] G. Raes, L. Brys, B.K. Dahal, J. Brandt, J. Grooten, F. Brombacher, G. Vanham, W. Noel, P. Bogaert, T. Boonefaes, A. Kindt, R. Van den Bergh, P.J. Leenen, P. De Baetselier, G.H. Ghassabeh, Macrophage galactose-type C-type lectins as novel markers for alternatively activated macrophages elicited by parasitic infections and allergic airway inflammation, Journal of leukocyte biology 77(3) (2005) 321-7.

[136] J.A. Vizcaino, A. Csordas, N. Del-Toro, J.A. Dianes, J. Griss, I. Lavidas, G. Mayer, Y. Perez-Riverol, F. Reisinger, T. Ternent, Q.W. Xu, R. Wang, H. Hermjakob, 2016 update of the PRIDE database and its related tools, Nucleic Acids Res 44(22) (2016) 11033.

FIGURE LEGENDS

Fig. 1 *In vitro* macrophage infection model with *L. donovani* promastigotes and SILAC-based macrophage proteomics analysis (A) Histogram plots showing the number of intracellular parasites per labeled and control macrophages after 4 h, 48 h and 72 h of infection. (B) Venn diagram showing the number of labeled proteins versus the number of non labeled proteins of differentiated macrophages in SILAC medium 6 days post-infection. (C) Workflow diagram showing the experimental strategy used to reveal the variable proteome of *L. donovani* infected BMDMs. Initially, an equal number of bone marrow (BM) progenitors were cultured and differentiated in the presence of natural amino acids (light “control” medium)

or amino acid with heavy isotopes (heavy "labeled" medium) supplemented with 75 ng/mL mCSF. After 6 days of differentiation, adherent cells were detached and plated with fresh control or labeled medium supplemented with 25 ng/mL mCSF. Labeled (red) and control (blue) macrophages were infected or not with stationary phase *L. donovani* promastigotes at a ratio of 10:1 for 4 h. Macrophages were lysed 72 h post-infection, protein extracts were quantified and mixed at a 1:1 ratio in pairs (control vs labeled, infected or not), fractionated by either polyacrylamide gel electrophoresis fractionation (GEL) or strong anion exchange fractionation (SAX), and processed by LC-MS/MS analysis. Error bars represent standard error of the mean (SEM).

Fig. 2 Summary of proteomics results (A) Venn diagram showing the overlap of identified proteins between L-I/C-NI and C-I/L-NI after GEL (left panel) or SAX fractionation (right panel). (B) Venn diagram showing the combined overlap identified proteins of L-I/C-NI, C-I/L-NI samples in both GEL and SAX fractionation conditions. (C) Volcano plots of the data presented in (A) showing the fold change (FC, x-axis, log2) of abundance for proteins with at least two identified peptides plotted against the p-value (y-axis, -log10). Red vertical and green horizontal lines reflect the filtering criteria, i.e. FC≥1.25 or FC≤0.8, and significance level of 0.05, respectively.

Fig. 3 Differential abundance for BMDM proteins and transcripts at 72 h post *L. donovani* infection (A) Immunoblot analysis. 20 µg of total protein extracts from infected (I) and non-infected (NI) BMDMs were analysed for Asah-1, Rab3IL1, Plxna1, Hmox-1, Gstm, and Ctsd proteins. β-actin expression was used as a loading control. The intensities of the bands were analysed using the Image J software. The fold overexpression, represented as a bar diagram, was calculated by dividing the band intensity representing the protein of interest with the band intensity of β-actin. Results are representative for three independent experiments. **, $p < 0.01$; *, $p < 0.05$, compared with the corresponding control value for noninfected macrophages (two-tail paired Student's t test). (B) RT-qPCR. Column diagrams showing the

mean ratio from three different experiments of RNA abundance in infected versus non-infected macrophages for Plxna1, Ppt1, Rab3IL1, Asah-1, Atp-7A and Hmox-1 relative to Ywhaz and RpL19. Error bars represent the standard deviations of three experiments.

Fig. 4 Gene Ontology analyses for up-regulated proteins in *L. donovani* infected BMDMs (A) GO analysis for Biological processes. (B) GO analysis for Molecular functions. (C) GO analysis for Cellular component. The analyses were performed using the hypergeometric statistical test, a Benjamini & Hochberg false discovery rate and significance level of 0.01. The p-value is indicated by the color according to the legend.

Fig. 5 Gene Ontology analyses for down-regulated proteins in *L. donovani* infected BMDMs. (A) GO analysis for Biological processes. (B) GO analysis for Molecular functions. (C) GO analysis for Cellular component. The analyses were performed using the hypergeometric statistical test, a Benjamini & Hochberg false discovery rate and significance level of 0.01. The p-value is indicated by the color according to the legend.

1153 **Table 1 Macrophage proteins displaying increased abundance after *L. donovani* infection**

Description	Uniprot ID	Gene	GEL:L-I/C-NI			GEL:C-I/L-NI		
			Ratio 1	p-value	No. Peptides	Ratio 2	p-value	No. Peptides
Glutamate--cysteine ligase regulatory subunit	O09172	Gclm	1.28	0.16	9	1.29	0.02	10
Complement component C1q receptor	O89103	Cd93	1.35	0.19	8	1.76	0.02	10
Fatty acid-binding protein, adipocyte	P04117	Fabp4	1.3	0.02	10	1.57	0.001	8
Urokinase-type plasminogen activator	P06869	Plau	6.02	0.04	5	5.41	0.003	6
Protein disulfide-isomerase A4	P08003	Pdia4	1.35	0.01	23	1.27	0.12	26
Ferritin heavy chain	P09528	Fth1	1.37	0.03	23	2.23	1.47E-07	20
Glutathione S-transferase Mu 1	P10649	Gstm1	1.36	0.003	26	2.53	8.21E-07	22
Integrin alpha-5	P11688	Itga5	1.34	0.001	18	1.27	0.3	18
Protein disulfide-isomerase A3	P27773	Pdia3	1.39	1.60E-08	51	1.27	7.97E-07	59
Ferritin light chain 1	P29391	Ftl1	2.9	3.90E-07	18	2.64	0.009	5
CD9 antigen	P40240	Cd9	1.41	0.16	5	1.76	0.004	6
Signal recognition particle receptor subunit beta	P47758	Srprb	1.36	0.04	7	1.25	0.14	8
V-type proton ATPase subunit D	P57746	Atp6v1d	1.29	0.31	9	1.37	0.003	6
40S ribosomal protein S15a	P62245	Rps15a	1.31	0.006	11	1.34	0.499	7
Histone H4	P62806	Hist1h4	1.55	3.40E-06	12	1.33	0.15	14

Plexin-A1	P70206	Plxna1	1.65	3.00E-05	35	2.46	1.81E-10	35
Keratin, type I cytoskeletal 9	Q6RHW0	Krt9	∞		8	∞		3
Sterol O-acyltransferase 1	Q61263	Soat1	1.29	0.13	10	1.31	0.03	13
Transmembrane protein 214	Q8BM55	Tmem214	1.34	0.04	5	1.87	0.21	7
Procollagen galactosyl-transferase 1	Q8K297	Glt25d1	2.53	0.12	8	1.5	0.001	11
Na+/K+-transporting ATPase subunit alpha-1	Q8VDN2	Atp1a1	1.39	0.001	17	1.26	0.007	22
Ribophorin I	Q91YQ5	Rpn1	1.65	0.0003	26	1.28	0.009	32
Protein disulfide-isomerase A6	Q922R8	Pdia6	1.43	0.0004	19	1.31	0.05	19
N-acylneuraminate cytidylyltransferase	Q99KK2	Cmas	1.27	0.37	11	1.72	0.002	10
BolA-like protein 1	Q9D8S9	Bola1	1.73	0.45	2	∞		2
Cap-specific mRNA (nucleoside-2'-O-)-methyltransferase 1	Q9DBC3	Cmtr1	1.39	0.72	2	∞		4
Hypoxia up-regulated protein 1	Q9JKR6	Hyou1	1.86	2.90E-05	36	1.38	0.008	45
Succinyl-CoA ligase [ADP-forming] subunit beta, mitochondrial	Q9Z2I9	Sucla2	1.27	0.48	10	1.37	0.007	17

Description	**Uniprot ID**	**Gene**	**GEL:L-I/C-NI**			**GEL:C-I/L-NI**		
			Ratio 1	**p-value**	**No. peptides**	**Ratio 2**	**p-value**	**No. peptides**
Phytanoyl-CoA dioxygenase, peroxisomal	O35386	Phyh	∞		2	1.25	0.53	2
26S protease regulatory subunit 6A	O88685	Psmc3	1.34	0.56	17	1.25	0.03	21
Glutathione S-transferase Mu 1	P10649	Gstm1	1.41	0.14	16	2.18	0.002	22

Amine oxidase [flavin-containing] A	Q64133	Maoa	1.31	0.54	15	2.24	0.005	15
Copper-transporting ATPase 1	Q64430	Atp7a	2.61	0.63	3	2.56	0.03	4
Protein PRRC2A	Q7TSC1	Prrc2a	∞		3	3.86	0.08	3
TBC1 domain family member 22A	Q8R5A6	Tbc1d22a	∞		2	1.89	0.48	3
Tumor necrosis factor alpha-induced protein 8-like protein 2	Q9D8Y7	Tnfaip8l2	∞		4	1.44	0.71	2

1154

Table 2 Macrophage proteins displaying decreased abundance after *L. donovani* infection

Description	Uniprot ID	Gene	GEL :L-I/C-NI			GEL: C-I/L-NI		
			Ratio 1	p-value	No. Peptides	Ratio 2	p-value	No. Peptide
Macrophage-expressed gene 1 protein	A1L314	Mpeg1	0.31	0.0006	12	0.4	1.00E-06	16
1.Transcription elongation factor SPT5	O55201	Supt5h	0.67	0.01	12	0.68	0.003	17
Integrin beta-5	O70309	Itgb5	0.73	0.31	9	0.55	0.01	5
Palmitoyl-protein thioesterase 1	O88531	Ppt1	0.23	0.001	8	0.3	2.00E-05	11
Tripeptidyl-peptidase 1	O89023	Tpp1	0.65	0.44	4	0.58	0.0181	8
Cathepsin B	P10605	Ctsb	0.59	4.00E-05	22	0.54	9.00E-08	22
Beta-glucuronidase	P12265	Gusb	0.69	9.00E-06	35	0.65	1.00E-05	32
Heme oxygenase 1	P14901	Hmox1	0.67	0.07	7	0.39	2.00E-06	15
Lysosome-associated membrane glycoprotein 2	P17047	Lamp2	0.72	0.04	9	0.7	0.4494	9
Cathepsin D	P18242	Ctsd	0.35	1.00E-13	35	0.59	4.00E-06	35
Ribosomal protein S6 kinase alpha-1	P18653	Rps6ka1	0.43	0.343	3	1/∞		2
Beta-galactosidase	P23780	Glb1	0.55	0.001	18	0.76	0.19	18
Lysosomal acid phosphatase	P24638	Acp2	0.41	0.003	5	0.75	0.36	4
Granulins	P28798	Grn	0.7	0.281	5	0.62	0.02	8
Beta-hexosaminidase subunit alpha	P29416	Hexa	0.74	0.009	20	0.62	0.02	21
Lamp4, Macrosialin	P31996	Cd68	0.68	0.006	8	0.49	0.07	8
Alpha-galactosidase	P51569	Gla	0.63	0.183	14	0.75	0.001	14
Erythrocyte band 7 integral membrane protein, Stomatin	P54116	Stom	0.78	0.057	11	0.48	0.01	6
Deoxyribonuclease-2-alpha	P56542	Dnase2	0.61	0.519	2	0.47	0.05	2
Acid sphingomyelinase-like phosphodiesterase 3a	P70158	Smpdl3a	0.44	0.0001	13	0.44	0.01	12
Dipeptidyl peptidase 1/ Cathepsin c	P97821	Ctsc	0.49	5.00E-05	14	0.41	0.004	10
Putative phospholipase B-like 2	Q3TCN2	Plbd2	0.71	0.009	11	0.49	0.05	9
Platelet-activating factor acetylhydrolase	Q60963	Pla2g7	0.68	0.2	6	0.35	1.00E-05	11
Serine/threonine-protein phosphatase 2A 56 kDa regulatory subunit epsilon isoform	Q61151	Ppp2r5e	1/∞		3	0.73	0.14	3
Macrophage mannose receptor 1	Q61830	Mrc1	0.63	1.00E-05	37	0.33	9.00E-16	41
CD180 antigen	Q62192	Cd180	0.66	0.012	15	0.76	0.0246	16
Transcription elongation factor SPT6	Q62383	Supt6h	0.59	0.018	7	0.64	0.02	7
Pseudopodium-enriched atypical kinase 1	Q69Z38	Peak1	0.45	0.127	6	0.47	0.01	9

Structural maintenance of chromosomes flexible hinge domain-containing prot. 1	Q6P5D8	Smchd1	0.66	0.172	12	0.51	8,00E-05	15
GEM-interacting protein	Q6PGG2	Gmip	0.79	0.48	7	0.49	0.004	9
Toll-like receptor 13	Q6R5N8	Tlr13	0.66	0.012	15	0.5	8.00E-06	20
E3 ubiquitin-protein ligase UBR2	Q6WKZ8	Ubr2	0.61	0.018	2	0.67	0.014	5
Nischarin	Q80TM9	Nisch	0.66	0.026	17	0.46	6.00E-07	25
ATP-dependent RNA helicase DDX42	Q810A7	Ddx42	0.74	0.122	10	0.65	0.02	7
Guanine nucleotide exchange factor for Rab-3A	Q8VDV3	Rab3il1	0.66	0.144	4	0,29	0.001	6
Beta-arrestin-2	Q91YI4	Arrb2	0.61	0.169	9	0.4	0.05	7
Leupaxin	Q99N69	Lpxn	0.74	0.049	12	0.65	0.003	12
Dipeptidyl peptidase 2	Q9ET22	Dpp7	0.4	0.011	8	0.75	0.23	6
Peptidyl-prolyl cis-trans isomerase NIMA-interacting 1	Q9QUR7	Pin1	0.68	0.198	5	0.5	0.04	3
Integrin alpha-X	Q9QXH4	Itgax	1/∞		2	0.33	0.001	4
Eukaryotic translation initiation factor 3 subunit I	Q9QZD9	Eif3i	0.77	0.399	6	0.73	0.03	9
Acid ceramidase	Q9WV54	Asah1	0.45	5.00E-06	15	0.5	0.1	14

Description	**Uniprot ID**	**Gene**	**SAX:L-I/C-NI**			**SAX:C-I/L-NI**		
			Ratio 1	**p-value**	**No. Peptides**	**Ratio 2**	**p-value**	**No. Peptide**
Macrophage-expressed gene 1 protein	A1L314	Mpeg1	0.43	0.32	7	0.45	0.01	6
Palmitoyl-protein thioesterase 1	O88531	Ppt1	0.29	0.03	7	0.22	0.02	8
Beta-2-microglobulin	P01887	B2m	0.61	0.39	4	1/∞		2
Cathepsin D	P18242	Ctsd	0.30	9.90E-07	26	0.77	0.21	20
Acid sphingomyelinase-like phosphodiesterase 3a	P70158	Smpdl3a	0.50	0.03	12	0.80	0.38	10
Caspase-7	P97864	Casp7,Lice2	0.69	0.56	4	0.69	0.03	3
Ral guanine nucleotide dissociation stimulator-like 2	Q61193	Rgl2,Rab2l, Rlf	1/∞		2	0.71	0.74	2
Macrophage mannose receptor 1	Q61830	Mrc1	0.67	0.09	24	0.31	0.01	17
60S ribosomal protein L10	Q6ZWV3	Rpl10,Qm	0.35	0.7	4	0.6	0.01	3
G-protein coupled receptor 84	Q8CIM5	Gpr84	1/∞		3	1/∞		2
Arfaptin-2	Q8K221	Arfip2	1/∞		2	0.64		1

	tRNA-dihydrouridine(47) synthase [NAD(P)(+)]-like	Q91XI1	Dus3l	1/∞	2	0.68	0.60	2
	Transmembrane 9 superfamily member 1	Q9DBU0	Tm9sf1	1/∞	2	0.64	0.76	2

1156

1157

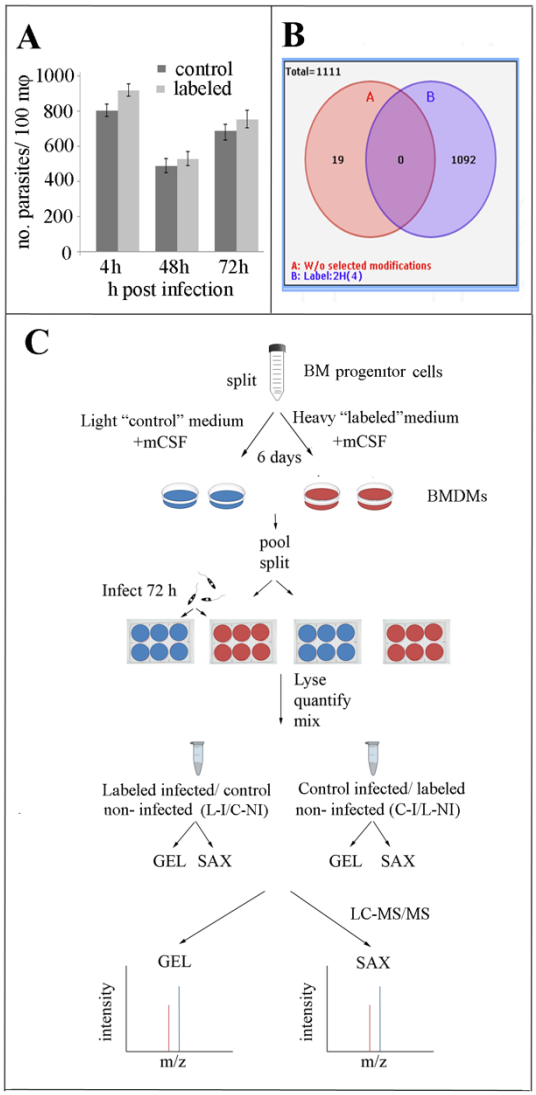
A
control
labeled
no. parasites/ 100 mφ
1000
800
600
400
200
0
4h
48h
72h
h post infection
B
Total=1111
A
B
19
0
1092
A: W/o selected modifications
B: Label:2H(4)
C
split
BM progenitor cells
Light "control" medium
+mCSF
Heavy "labeled"medium
+mCSF
6 days
BMDMs
pool
split
Infect 72 h
Lyse
quantify
mix
Labeled infected/ control
non- infected (L-I/C-NI)
Control infected/ labeled
non- infected (C-I/L-NI)
GEL
SAX
GEL
SAX
LC-MS/MS
GEL
SAX
intensity
m/z
intensity
m/z

Figure 1

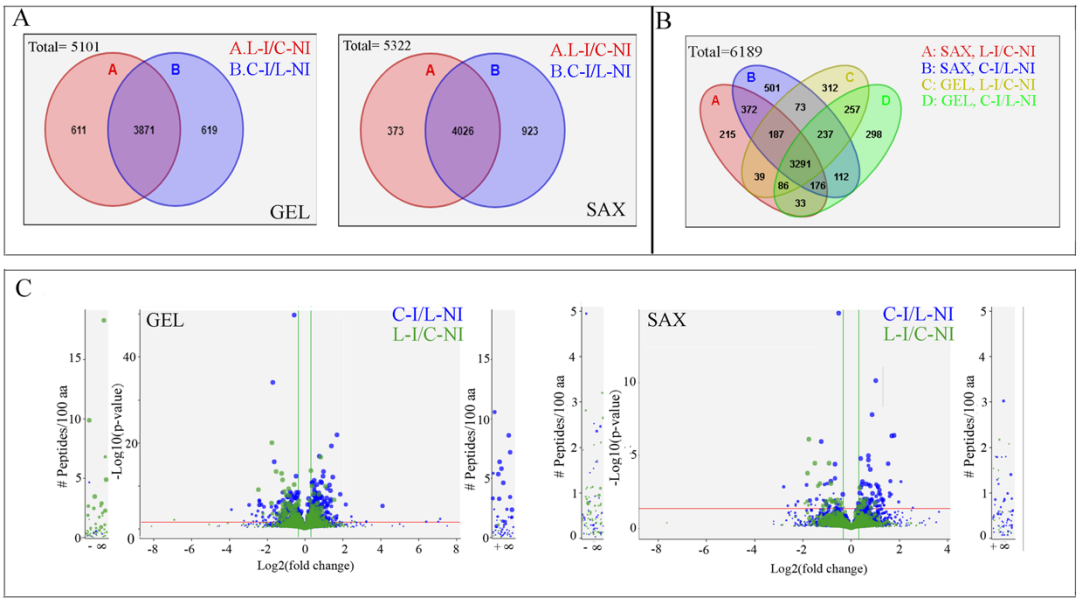

1159 **Figure 2**

1160 **Figure 3**

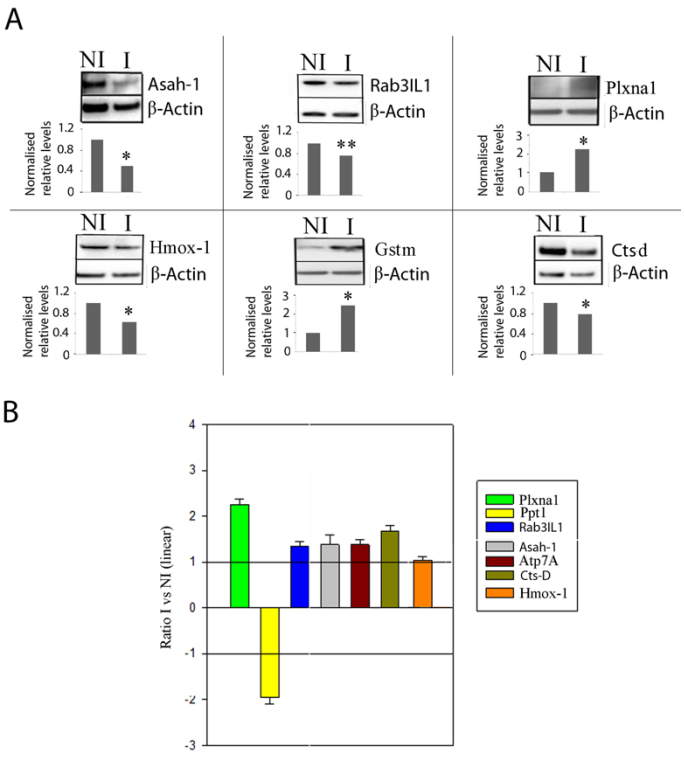

1161 **Figure 4**

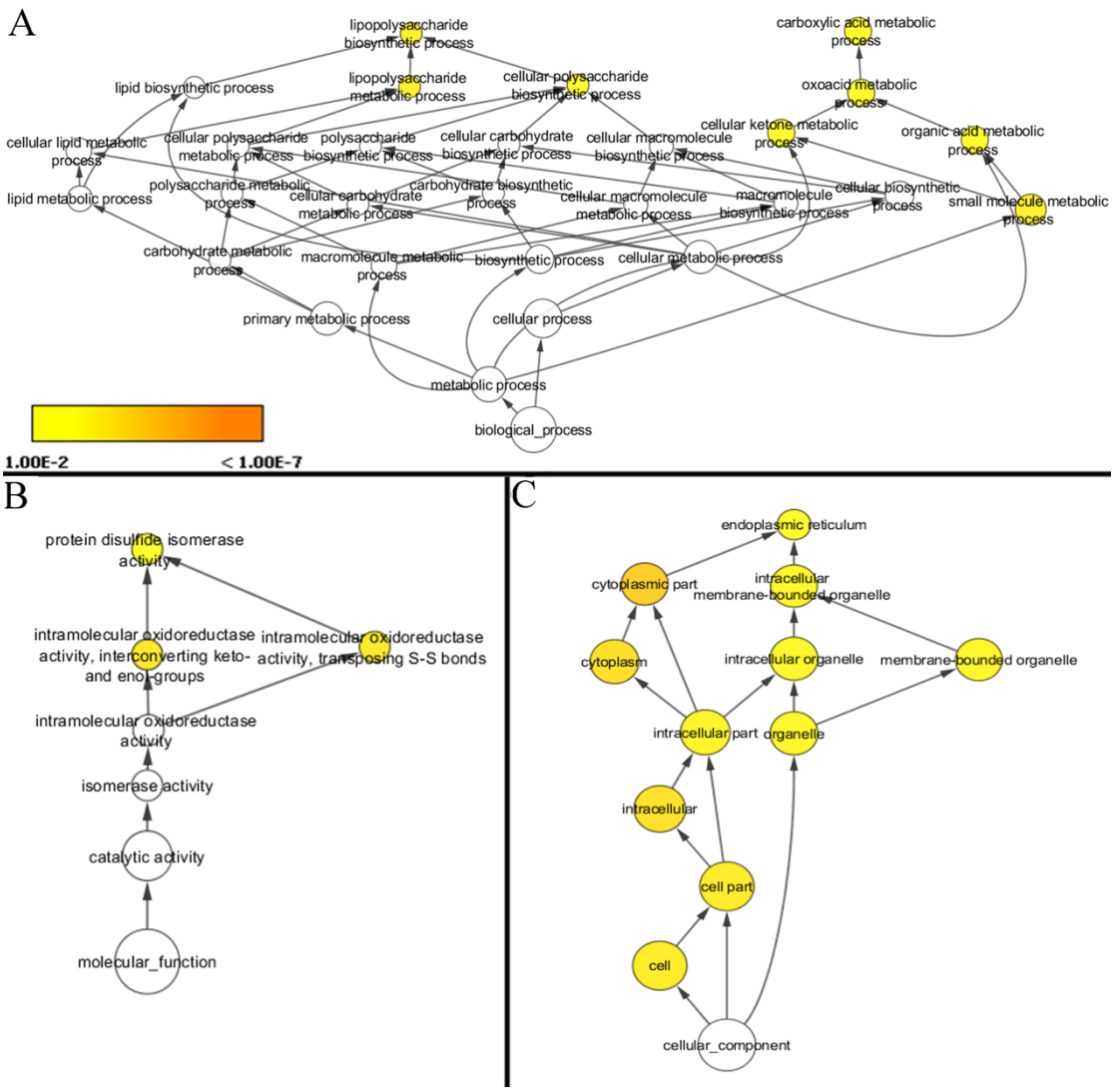

1162 **Figure 5**

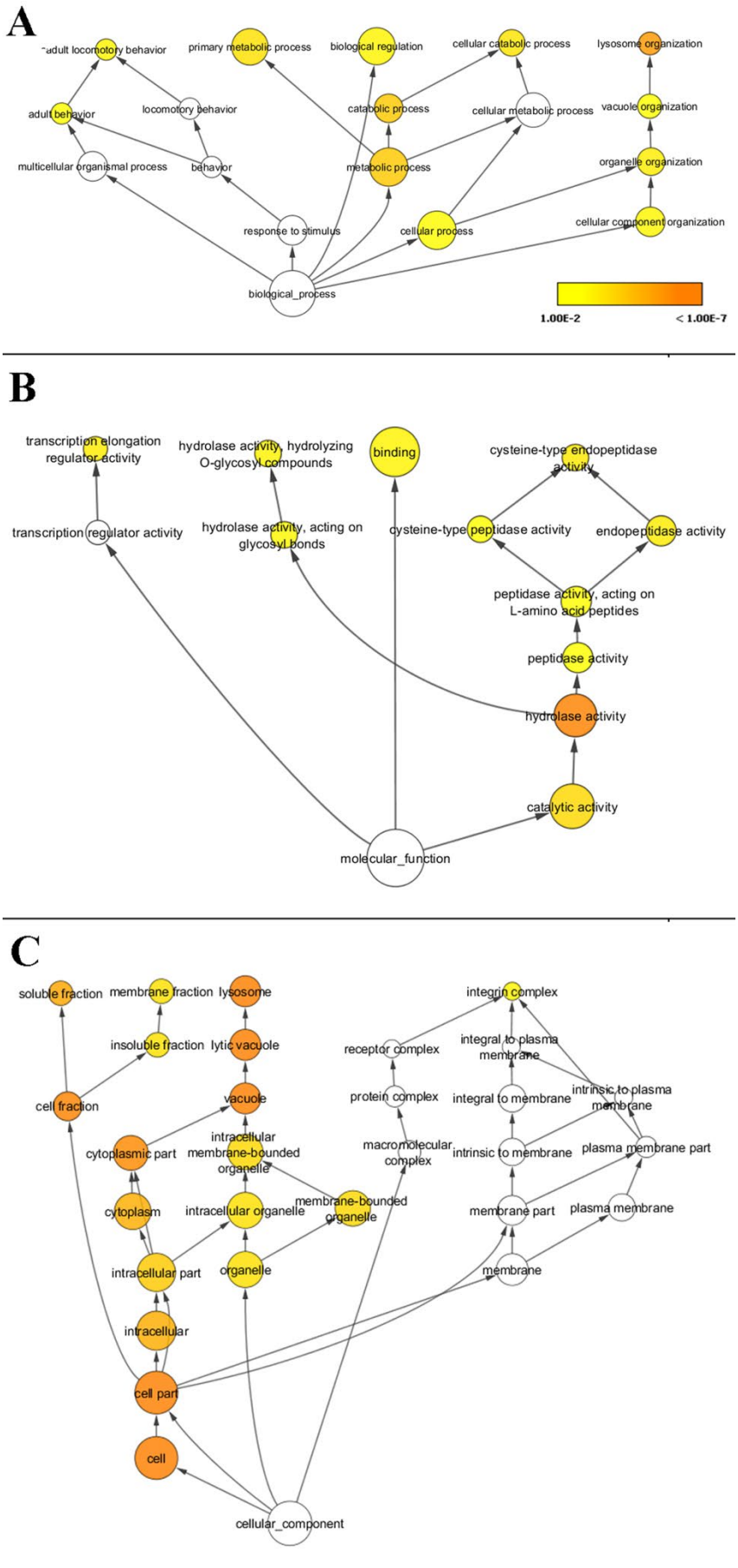

1163